Projections of Heat Stress in Vietnam Using Physically-Projections of Heat Stress in Vietnam Using Physically-Based Wet-Bulb Globe Temperature

Dzung Nguyen-Le, Long Trinh-Tuan, Thanh Nguyen-Xuan, Tung Nguyen-Duy, Thanh Ngo-Duc, Marie-Noëlle Woillez

MAY 2025
No. 346

Authors
Dzung Nguyen-Le
Long Trinh-Tuan
Thanh Nguyen-Xuan
Tung Nguyen-Duy
Thanh Ngo-Duc
Coordination
Marie-Noëlle Woillez (AFD)

Research papers

Projections of Heat Stress in Vietnam Using Physically-Based Wet-Bulb Globe Temperature

ÉDITIONS AFD
AGENCE FRANÇAISE DE DÉVELOPPEMENT

Agence française de développement

Papiers de recherche

Les *Papiers de Recherche de l'AFD* ont pour but de diffuser rapidement les résultats de travaux en cours. Ils s'adressent principalement aux chercheurs, aux étudiants et au monde académique. Ils couvrent l'ensemble des sujets de travail de l'AFD : analyse économique, théorie économique, analyse des politiques publiques, sciences de l'ingénieur, sociologie, géographie et anthropologie. Une publication dans les *Papiers de Recherche de l'AFD* n'en exclut aucune autre.

Les opinions exprimées dans ce papier sont celles de son (ses) auteur(s) et ne reflètent pas nécessairement celles de l'AFD. Ce document est publié sous l'entière responsabilité de son (ses) auteur(s) ou des institutions partenaires.

Research Papers

AFD Research Papers are intended to rapidly disseminate findings of ongoing work and mainly target researchers, students and the wider academic community. They cover the full range of AFD work, including: economic analysis, economic theory, policy analysis, engineering sciences, sociology, geography and anthropology. *AFD Research Papers* and other publications are not mutually exclusive.

The opinions expressed in this paper are those of the author(s) and do not necessarily reflect the position of AFD. It is therefore published under the sole responsibility of its author(s) or its partner institutions.

Projections of Heat Stress in Vietnam Using Physically-Based Wet-Bulb Globe Temperature

AUTHORS

Dzung Nguyen-Le*
Department of Space and Applications, University of Science and Technology of Hanoi (USTH), Vietnam Academy of Science and Technology (VAST), Hanoi, Vietnam

Long Trinh-Tuan
Vietnam Academy Water and Resources, Hanoi, Vietnam

Thanh Nguyen-Xuan
Department of Space and Applications, University of Science and Technology of Hanoi (USTH), Vietnam Academy of Science and Technology (VAST), Hanoi, Vietnam

Tung Nguyen-Duy
Oxford University Clinical Research Unit, Ho Chi Minh city, Vietnam

Thanh Ngo-Duc
Department of Space and Applications, University of Science and Technology of Hanoi (USTH), Vietnam Academy of Science and Technology (VAST), Hanoi, Vietnam

COORDINATION

Marie-Noëlle Woillez (AFD)

* Corresponding author
nguyen-le.dung@usth.edu.vn

Abstract
The wet-bulb globe temperature (WBGT) is a widely used index for assessing heat stress. However, many studies on heat stress under climate change rely on simplified WBGT calculations, which may introduce biases. In this study, high-resolution climate data and the physically-based WBGT model are employed to provide a more reliable assessment of future heat stress impacts across Vietnam and its seven sub-climatic regions. Projected changes are analyzed for three future periods — the near future (2021–2040), mid-future (2041–2060), and far future (2081–2100) — relative to the baseline period (1995–2014) under three Shared Socioeconomic Pathways (SSPs): SSP1-2.6, SSP2-4.5, and SSP5-8.5. Additionally, changes are assessed across different global warming levels (GWL), ranging from 1.5°C to 4°C above the pre-industrial level. Long-term trends throughout the studied period are also examined. The findings reveal significant increases in heat stress across Vietnam in the future. A major concern is the substantial increases in the number of days exceeding impact-relevant heat stress thresholds, most notably in the Red River Delta and Mekong River Delta, two most densely populated and agriculturally critical sub-regions of Vietnam. Heat stress emergence and intensity are closely linked to the radiative forcing of SSP scenarios and the GWLs, with higher forcing scenarios and warmer GWL producing more severe conditions and a greater frequency of exceedance days. The most severe impacts are projected under SSP5-8.5 as well as GWLs of 3°C and 4°C, indicating the urgent need to limit future warming to mitigate the risk of heat stress. Biases in simplified WBGT calculations are also discussed, suggesting significant overestimations of exceedance days in most of Vietnam. Such biases could lead to misleading assessments, unnecessary alarms, and potentially flawed adaptation strategies, highlighting the critical need for accurate WBGT modeling in climate impact research.

Keywords
Climate Change, heat stress, WBGT, Global Warming Level, Vietnam

Acknowledgements
This study is supported by the 2nd phase of the GEMMES Vietnam project, funded by the French Development Agency (AFD) through Facility 2050, and by the Vietnam Academy of Science and Technology (VAST) under Grant THTETN.01/25-26. The down-scaled CMIP6 data were obtained from the SEACLID/ CORDEX-SEA project funded by the Asia Pacific Network for Global Change Research (CRRP2023-658 08MY-Cruz) and by the Vietnam National Foundation for Science and Technology Development (NAFOSTED) under Grant 105.06-2021.14. We would like to express our special thanks to Dr. Marie-Noëlle Woillez from AFD for her careful review and valuable suggestions to improve this manuscript.

Original version
English

Accepted
April 2025

Résumé
La température au globe humide (WBGT) est un indice largement utilisé pour évaluer le stress thermique. Cependant, de nombreuses études sur le stress thermique dans le contexte du changement climatique s'appuient sur des calculs simplifiés du WBGT, ce qui peut introduire des biais. Dans cette étude, des données climatiques à haute résolution et un modèle WBGT basé sur la physique sont utilisés afin de fournir une évaluation plus fiable des impacts futurs du stress thermique au Vietnam et dans ses sept sous-régions climatiques. Les changements projetés sont analysés pour trois périodes futures — le futur proche (2021–2040), le milieu du siècle (2041–2060) et le futur lointain (2081–2100) — par rapport à la période de référence (1995–2014) sous trois scénarios de trajectoires socio-économiques partagées (SSP) : SSP1-2.6, SSP2-4.5 et SSP5-8.5. De plus, les évolutions sont évaluées pour différents niveaux de réchauf-fement global (GWL), allant de 1,5°C à 4°C au-dessus du niveau préindustriel. Les tendances à long terme sur l'ensemble de la période étudiée sont également examinées. Les résultats révèlent une augmentation significative du stress thermique au Vietnam dans le futur. L'augmentation substantielle du nombre de jours dépassant des seuils critiques de stress thermique est particulièrement préoccupante, notamment dans le delta du fleuve Rouge et le delta du Mékong, les deux sous-régions les plus densément peuplées et cruciales pour l'agriculture du pays. L'émergence et l'intensité du stress thermique sont étroitement liées au forçage radiatif des scénarios SSP et aux niveaux de réchauffement global, les scénarios à fort forçage et les GWL les plus élevés produisant des conditions plus sévères et une fréquence accrue de jours de dépassement des seuils critiques. Les impacts les plus sévères sont projetés pour le scénario SSP5-8.5 ainsi qu'aux niveaux de réchauffement de 3°C et 4°C, soulignant l'urgence de limiter le réchauffement futur pour atténuer les risques liés au stress thermique. Les biais des calculs simplifiés du WBGT sont également discutés, suggérant une surestimation significative du nombre de jours de dépassement dans la majeure partie du Vietnam. De tels biais pourraient conduire à des évaluations trompeuses, des alarmes inutiles et des stratégies d'adaptation potentiellement erronées, mettant en évidence la nécessité cruciale d'une modélisation précise du WBGT dans la recherche sur les impacts climatiques.

Mots-clés
Changement climatique, stress thermique, WBGT, niveau de réchauffement global, Vietnam

Remerciements
Cette étude est soutenue par la deuxième phase du projet GEMMES Vietnam, financé par l'Agence Française de Développement (AFD) via la Facilité 2050, et par l'Académie des Sciences et de la Technologie du Vietnam (VAST) dans le cadre de la subvention THTETN.01/25-26. Les données réduites du CMIP6 ont été obtenues dans le cadre du projet SEACLID/CORDEX-SEA, financé par le Réseau Asie-Pacifique pour la recherche sur le changement global (CRRP2023-658 08MY-Cruz) et par la Fondation nationale pour le développement de la science et de la technologie du Vietnam (NAFOSTED) sous la subvention 105.06-2021.14. Nous souhaitons exprimer nos remerciements spéciaux au Dr. Marie-Noëlle Woillez de l'AFD pour sa relecture attentive et ses précieuses suggestions visant à améliorer ce manuscrit.

Version originale
Anglais

Acceptée
Avril 2025

Introduction

Heat stress has been identified as a leading cause of weather-related deaths (Barriopedro *et al.*, 2011; Buzan *et al.*, 2015) and has broad social and economic impacts, including reduced agricultural productivity, increased healthcare costs, and decreased labor productivity (*e.g.* Barriopedro *et al.*, 2011; Dunne et al 2013; Kjellstrom *et al.* 2016; Schleussner *et al.*, 2016; Maia-Silva *et al.* 2020; Orlov *et al.* 2020; Shen *et al.* 2020; Ebi *et al.* 2021). It is projected to become an even more significant threat in the future under global warming (*e.g.* Sherwood and Huber 2010; Diffenbaugh and Giorgi 2012; Willett and Sherwood 2012; Im *et al.* 2017; Buzan and Hubner 2020; Li *et al.* 2020; Schwingshackl *et al.* 2021).

To quantify heat stress, various heat stress indices have been proposed. Nevertheless, only a limited subset of these indices is suitable for evaluating the impacts of climate change (de Freitas and Grigorieva 2017). Among them, the wet-bulb globe temperature (WBGT) is widely used due to its straightforward physical interpretation, incorporation of all four key ambient factors contributing to heat stress (temperature, humidity, wind, and radiation), and established safety thresholds for activity adjustments (*e.g.* ISO 2017). Despite its advantages, the WBGT measurement is resource-intensive, requiring specialized instruments and skilled operators. To address these limitations, various simplified methods have been proposed to approximate WBGT using standard meteorological data. However, recent studies have criticized such simplifications for their inaccuracies (*e.g.* Jacobs *et al.* 2019; Kong and Huber 2022; Qiu *et al.* 2024). Kong and Huber (2022) show that simplified WBGT significantly overestimates heat stress in hot-humid regions and underestimates it in arid regions. Qiu *et al.* (2024) further suggest that simplified WBGT overestimates the increase in heat stress levels under future warming scenarios, with the degree of overestimation strongly correlated with local climatological temperature. They emphasize the need for using physically-based WBGT calculations with high-resolution climate data for more reliable heat stress assessments in climate change research.

Located in tropical Southeast Asia, Vietnam is among the countries most severely impacted by climate change (UNFCCC 2007). Its wide longitudinal range and complex terrain require high-resolution climate projections for effective adaptation and mitigation strategies. Based on Global Climate Models (GCMs) from Phase 6 of the Coupled Model Intercomparison Project (CMIP6; Eyring *et al.*, 2016), Schwingshackl *et al.* (2021)

project significant increases in heat stress over Southeast Asia throughout this century. However, the coarse spatial resolution of CMIP6 GCMs, typically 100–200 km, restricts their ability to accurately represent regional climate variability in Vietnam (Desmet and Ngo-Duc, 2022). To address this limitation, the Coordinated Regional Downscaling Experiment-Southeast Asia (CORDEX-SEA) project (Tangang *et al.*, 2020; Ngo-Duc *et al.*, 2024) dynamically downscales a suite of CMIP6 GCMs to a high-resolution grid of 25 km. This dataset, which extends through the end of the 21st century under the latest Shared Socio-economic Pathways (SSPs) (O'Neill *et al.*, 2017), provides a valuable opportunity for comprehensive assessments of heat stress impacts in Vietnam using multi-model, and multi-scenario frameworks.

Recent studies in Vietnam have examined heat stress in major cities like Hanoi (Hoang *et al.* 2022), Ho Chi Minh City (Dang et al. 2019), other urban areas (Phung *et al.* 2017), and the entire country (Vu and Ngo-Duc 2024). These studies consistently report increasing heat stress over recent decades with notable socio-economic implications. However, their focus is on historical variations without providing projections under global warming. Further, they rely on simplified heat stress indices based only on daily air temperature and humidity, which are less effective for assessing outdoor heat stress, particularly under high solar radiation conditions. Importantly, none of these results incorporate critical heat stress thresholds that directly impact human health and well-being. Tropical regions are particularly vulnerable to heat stress, which is a growing health hazard in areas lacking adequate health surveillance and intervention systems (Gao *et al.* 2019). Given the high prevalence of outdoor activities in Vietnam, accurate assessments of heat stress impacts require physically-based models. The WBGT model developed by Liljegren *et al.* (2008) is highly sophisticated, based on standard meteorological data, well-calibrated and validated (Liljegren *et al.* 2008; Lemke and Kjellstrom 2012). This study projects future changes in heat stress across Vietnam and its seven sub-climatic regions using Liljegren's model with high-resolution climate data for explicit calculation of WBGT. The calculated WBGT values will be linked to critical heat stress thresholds directly relevant to human health. To the best of our knowledge, this is the first application of such an approach in Vietnam and Southeast Asia. The results provide valuable insights into the socio-economic and health implications of heat stress, offering essential guidance for policy-makers to develop effective climate change adaptation and mitigation strategies.

This paper is organized as follows. Section 2 provides a brief description of the study regions, the calculation of WBGT,

its impact-relevant thresholds, and data sources. Section 3 presents the main results and related discussions. Finally, Section 4 draws conclusions.

1. Studied regions, Data and Methods

1.1. Studied regions

This study focuses on Vietnam, specifically examining its seven sub-climatic regions (Figure 1). These subregions — Northwest (R1), Northeast (R2), Red River Delta (R3), North Central (R4), Central South (R5), Central Highlands (R6), and Southern (R7) — are categorized based on variations in radiation, temperature, and rainfall, with the North domain (R1-R4) differing from the South domain (R5-R7) in terms of radiation and temperature, while rainfall further differentiates subregions within each domain (Nguyen and Nguyen, 2004).

Figure 1. Map of Vietnam and location of the seven sub-climatic regions

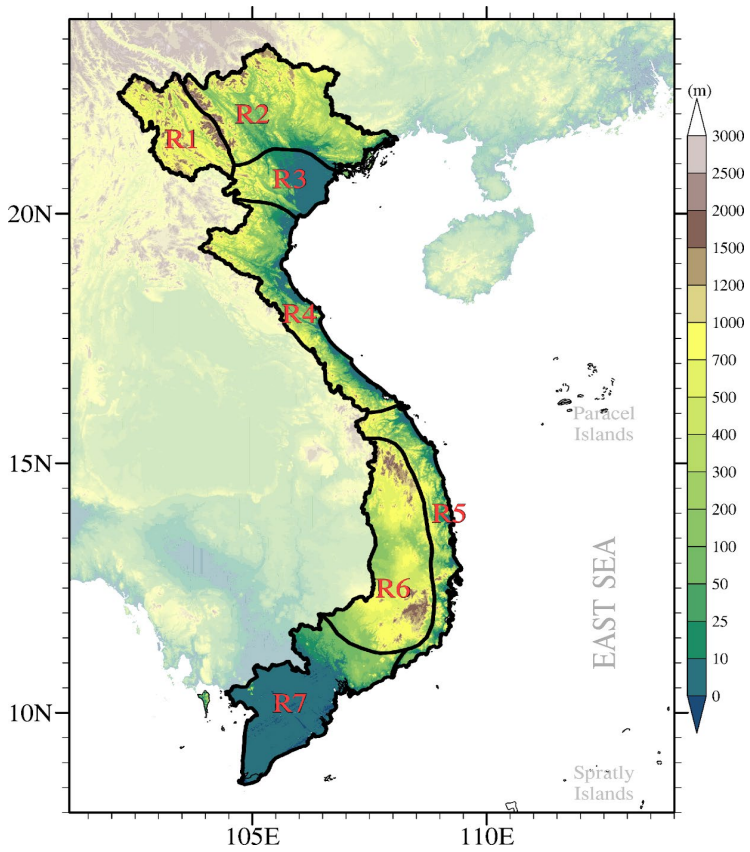

Source: Authors' own visualization. Original. Topography data (in color) is extracted from Hydroshed data (NASA SRTM 2013).

1.2. Heat stress index: WBGT estimated from Liljegren's Model

WBGT was developed by US military ergonomists in the 1950s. This index is widely used and recognized to assess heat stress conditions, especially for working people. It is calculated as a weighted average of three temperature measurements: natural wet-bulb temperature (T_w), black globe temperature (T_g), and dry bulb temperature (T_a) (Yaglou and Minard 1957). T_w is measured with a wetted thermometer exposed to the wind and heat radiation at the site. It simulates the cooling of the body via sweat evaporation and strongly depends on air temperature and humidity, but also on heat radiations and wind speed. T_g is measured inside a black globe and simulates the heat absorption from short- and long-wave radiations, i.e. from the sun, the soil or from other heat sources in the workplace. It depends on both the air temperature and wind speed. T_a corresponds to the air temperature, measured with a "normal" thermometer, shaded from direct heat radiations.

The specific equation used depends on the environment. For daytime condition in outdoor environment exposed to direct solar radiations, the calculation is:

$$WBGT_{outdoor} = 0.7T_w + 0.2T_g + 0.1T_a \quad (1)$$

For nighttime condition, indoor environment, or outdoor shaded areas (*i.e.*, without direct solar radiation), the equation is:

$$WBGT_{indoor} = 0.7T_w + 0.3T_g \quad (2)$$

Liljegren's model is a physically-based model that incorporates fundamental principles of heat and mass transfer to approximate WBGT. Detailed descriptions and equations of the model are given in Appendix A1. Liljegren (*et al.* 2008) provided their original code, which we utilized here in a Python implementation by Kong and Huber (2022). Daily maximum $WBGT_x$ and daily minimum $WBGT_m$ values are defined as the daily maximum of $WBGT_{outdoor}$ (Equation 1) and daily minimum of $WBGT_{indoor}$ (Equation 2), respectively.

1.3. Impact-Relevant Thresholds

Analyzing changes in heat stress indices alone may not directly translate to societal impacts, as these values vary based on the specific scales and definitions used. To better assess the societal implications of heat stress, impact-relevant thresholds are utilized.

Although epidemiological studies often lack specific absolute thresholds for heat stress, established benchmarks from occupational and athletic health safety regulations, as well as meteorological heat warning systems, provide a practical framework (Blazejczyk *et al.*, 2012; Kjellstrom *et al.*, 2009; Grundstein *et al.*, 2015; Zhao *et al.*, 2015). Following a previous study (Schwingshackl *et al.*, 2021), WBGT is categorized into four impact-relevant levels (see Table 1), adopting the threshold framework from Kjellstrom *et al.*, (2009). These thresholds describe heat impacts on workers during sustained moderate activity, *i.e.* an approximate metabolic rate of 300 Watts.

Table 1. Overview of the WBGT thresholds used in this study, distinguishing between four different severity levels

Levels	Thresholds	Recommendations	Assessment base
Level 1	29 °C	25% rest/hour	Recommended maximum WBGT exposure levels for medium work (~300 W) and rest/work ratios for an average acclimatized worker with light clothing. Source: Kjellstrom *et al.* (2009)
Level 2	30.5 °C	50% rest/hour	
Level 3	32 °C	75% rest/hour	
Level 4	37 °C	No work at all (100% rest/hour)	

1.4. Data

In this study, two types of datasets are used: reanalysis and climate model projections. The reanalysis data from ECMWF-ERA5 (Hersbach *et al.*, 2020) are used for calculating WBGT for the period of 1985–2014, serving as a reference for the bias correction procedure. Climate projections are obtained from the outputs of two CMIP6 GCMs (NorESM2-MM and CNRM-ESM2-1, see Table 2), dynamically downscaled over the CORDEX-SEA domain to a resolution of 25 km (Tangang *et al.*, 2020). These downscaled datasets are generated using the non-hydrostatic version of the ICTP Regional Climate Model (RCM), RegCM4-NH (Coppola *et al.*, 2021). For more information on the RegCM4-NH configuration, refer to Ngo-Duc *et al.* (2024). Note that the Equilibrium Climate Sensitivity (ECS) of NorESM2 is 2.5°C, i.e. at the lower end of the "likely" range of ECS (2.5°C-4°C) assessed in the Sixth Assessment Report (AR6) of IPCC (2021), while the ECS of CNRM-ESM2 is 4.76°C (Bock *et al.*, 2020), i.e. at the high end of the IPCC "very likely" range (2°C-5°C).

Three SSPs scenarios (SSP1-2.6, SSP2-4.5, and SSP5-8.5) are analyzed to represent a range of global greenhouse gas emission scenarios. In these scenarios, global temperature would rise by 1.8°C, 2.7°C and 4.4°C respectively above pre-industrial level by the end of the century (IPCC,2021). The baseline period spans 1995–2014 (20-year), while the future period extends from 2015 to 2100. The future period is further divided into three sub-periods: near future (2021–2040), mid-future (2041–2060), and far future (2081–2100).

Table 2. List of two CMIP6 GCMs used in the dynamical downscaling

N°	GCM	Original Resolution (lat. × lon.)	Member Variant	Equilibrium Climate Sensitivity (ECS)
1	NorESM2-MM	1.25°×0.94°	r1i1p1f1	2.5°C
2	CNRM-ESM2-1	1.41°×1.40°	r1i1p1f1	4.76°C

For WBGT calculations, several variables are required, including 2-meter near-surface air temperature (T_a), 2-meter relative humidity (*RH*), 10-meter wind speed (*WS*), surface downwelling shortwave radiation (*RSDS*), and surface air pressure (*PS*). These variables are extracted from all RCM outputs and ERA5 at a 3-hourly temporal resolution. Since *RH* is not directly provided in ERA5, near-surface dew point temperature (T_d) is used together with T_a to derive *RH* by August–Roche–Magnus approximation. To ensure consistency, all RCM outputs are spatially interpolated onto the 0.25° × 0.25° latitude–longitude grid of ERA5. Subsequently, all calculations are conducted separately for each RCM, and the results from the mean of the two RCM experiments are presented.

In addition, following the approach of IPCC AR6 and Hausfather *et al.* (2022), we complement scenario-based projections with GWL-based analyses. This method is justified by the strong relationship between climate variable changes (*e.g.*, temperature, precipitation) and GWL, regardless of the emission pathway or timing of threshold exceedance (IPCC, 2021). GWLs of 1.5°C, 2°C, 3°C, and 4°C are defined relative to the period 1850–1900, with YGWL representing the year when the 20-year centered average of the the global mean surface air temperature anomaly series first exceeds each threshold. The GWL periods for the two GCMs and three SSP scenarios used in this study follow Hauser *et al.* (2022), applying a 20-year window spanning 10 years before and 9 years after YGWL. Results are presented as the average across models and scenarios reaching a given GWL.

1.5. Bias correction

As climate models inevitably exhibit biases, a bias correction procedure is applied to adjust the calculated WBGT derived from simulations and projections. We employ the quantile delta mapping (QDM) approach described by Cannon *et al.* (2015) to match the distributions of RCM outputs during the application period to those of the ERA5 reanalysis during the historical period (1985–2014). By considering distributional changes between the reference and future periods for each quantile, QDM can accurately capture shifts in heat extremes while minimizing the risk of introducing artificial trends (Cannon *et al.* 2015; Maraun 2016). QDM is applied to daily maximum and minimum WBGT distributions of the ensemble mean at every grid point separately and for each month of the year individually. We utilized 50 quantiles for QDM, which is a balance between flexibility and the risk of overfitting (Zscheischler *et al.* 2019).

2. Results and Discussions

2.1. Projected future changes in WBGT across Vietnam

During the baseline period (1995–2014), the simulated climatological annual maximum WBGTx (WBGTx,x) already exceeded the Level 3 (>32°C) across Vietnam. It even surpasses the Level 4 (>37°C) in many areas of R3, R4, R5, western R2, central R6, and certain northwestern areas of R7 (Figure 2(a)). Projections for all future periods suggest significantly (p-value<0.05) warmer WBGTx,x across nearly all subregions. The lowest increases are projected under SSP1-2.6 (Figures 2(b)–(d)), and the highest are obtained under SSP5-8.5 (Figures 2(h)–(j)). More specifically, meanwhile the differences between scenarios remain modest in the near future (2021–2040), scenario-dependent variations become more pronounced in the mid- (2041–2060) and far future (2081–2100). Spatially, projected changes in WBGTx,x in the far future under lower emission scenarios resemble those in the mid-future under higher emission scenarios, such as the similarity between Figures 2(d) and 2(f) and between 2(g) and 2(i). In the near future, increases in WBGTx,x relative to the baseline period are generally less than 1°C across Vietnam, regardless of the scenarios. Under SSP1-2.6, WBGTx,x increases mildly by around 1°C in the mid-future and less than 2°C in the far future (Figures 2(c) and 2(d)). Slightly higher increases are projected under the "warmer" SSP2-4.5, with WBGTx,x increases around 2°C from the mid- to far future (Figures 2(f) and 2(g)). Unsurprisingly, the most pronounced increases are projected in the far future under SSP5-8.5, generally exceeding 2°C and possibly surpassing 3°C in central R6, northernmost R2, and southwestern R7 (Figure 2(j)). Additionally, significant (p-value<0.05) increasing trends in WBGTx,x of approximately 0.2, 0.3 and 0.4°C per decade are projected across Vietnam under SSP1-2.6, SSP2-4.5, and SSP5-8.5, respectively, during the entire studied period (1985–2100) (Figure S1). Overall, it is suggested that WBGTx,x increases significantly over Vietnam by the end of this century, with the magnitude scaling with radiative forcing.

For quantifying increases in human heat stress due to climate change, exceedances of WBGTx beyond impact-relevant thresholds provides a more informative metric than actual values. Figure 3 shows the annual number of days (Nx,3) on which WBGTx exceeds the Level 3 (>32°C). During the baseline period, the average number Nx,3 is generally below 100 days per year (d/yr) across most subregions (Figure 3a). However, higher values are observed in northern R5, and particularly northwestern R7, where Nx,3 already reaches 120–140 d/yduring the baseline period. In contrast, Nx,3 are less than 20–40 dy/y in R1, northeastern R2, and R6. Similar to WBGTx,x, projected differences in Nx,3 between scenarios are relatively

small in the near future, but are increasingly significant in the mid- and far future (Figures 3(b)–(j)). Projected changes in the far future under lower emission scenarios also resemble those in the mid-future under higher emission scenarios. Moreover, projected Nx,3 increases scale with radiative forcing, highlighting the direct linkage between emission pathways and heat stress severity. Specifically, in the near future, increases in Nx,3 are less than 30 dy/y in R1–R6 and less than 60 dy/y in R7 under all scenarios. Under SSP1-2.6, increases in Nx,3 remain modest even in the far future, generally below 30 dy/y, except for R7, where increases range from 60 to 90 dy/y (Figure 3(d)). Under SSP2-4.5, increases are slightly higher, reaching 90 to 120 dy/y in R7, while only 30 to 60 dy/y in other subregions in the far future (Figure 3(g)). The largest increases occur under SSP5-8.5 in the far future, with 60 to 120 dy/y in R1–R6 and over 150 dy/y in R7 (Figure 3(j)). Significant (p-value<0.05) increasing trends of Nx,3 are obtained throughout the study period, with less than 5 days per decade (dy/dc) under SSP1-2.6, around 5 dy/dc under SSP2-4.5, and 5–10 dy/dc or slightly higher under SSP5-8.5 in R1–R6 (Figure S2). However, R7 shows much more significant trends, exceeding 15–20 dy/dc under SSP5-8.5.

Figure 4 further illustrates the projected increases in WBGTx characteristics at different GWLs relative to the baseline. Overall, both WBGTx,x and Nx,3 increases across Vietnam with the magnitude scaling linearly with GWL. The increases projected for GWLs 1.5°C and 2°C are comparable to those projected for the mid-future under SSP2-4.5 and SSP5-8.5, respectively, while the increases at GWLs 3°C and 4°C exceed those projected for the far future under the same SSP scenarios. Specifically, WBGTx,x, increases by approximately 1oC, 1–2oC, slightly above 2oC and nearly 3oC across Vietnam at the GWLs of 1.5°C, 2°C, 3°C and 4°C, respectively (Figures 4(a)–(d)). For Nx,3, the projected increases at these GWLs are generally below 30, 60, 90, and 120 d/yr, respectively, over most sub-regions, except for R7 (Figures 4(e)–(h)). In R7, Nx,3 increases by more than 60 and 90 d/yr at the GWLs of 1.5°C and 2°C, respectively, and typically exceeds 120 d/yr at GWLs of 3°C and higher.

Figure 2. **Climatological annual maximum $WBGT_x$ ($WBGT_{x,x}$)**
(a) Spatial distribution of climatological annual maximum WBGTx (WBGTx,x) over Vietnam during the baseline period (1995–2014) and its projected changes for the (b), (e), (h) near future (NF; 2021–2040); (c), (f), (i) mid-future (MF; 2041–2060); and (d), (g), (j) far future (FF; 2081–2100) under three Shared Socioeconomic Pathways (top) SSP1-2.6, (middle) SSP2-4.5, and (bottom) SSP5-8.5. Only significant differences (p-value<0.05) are plotted.

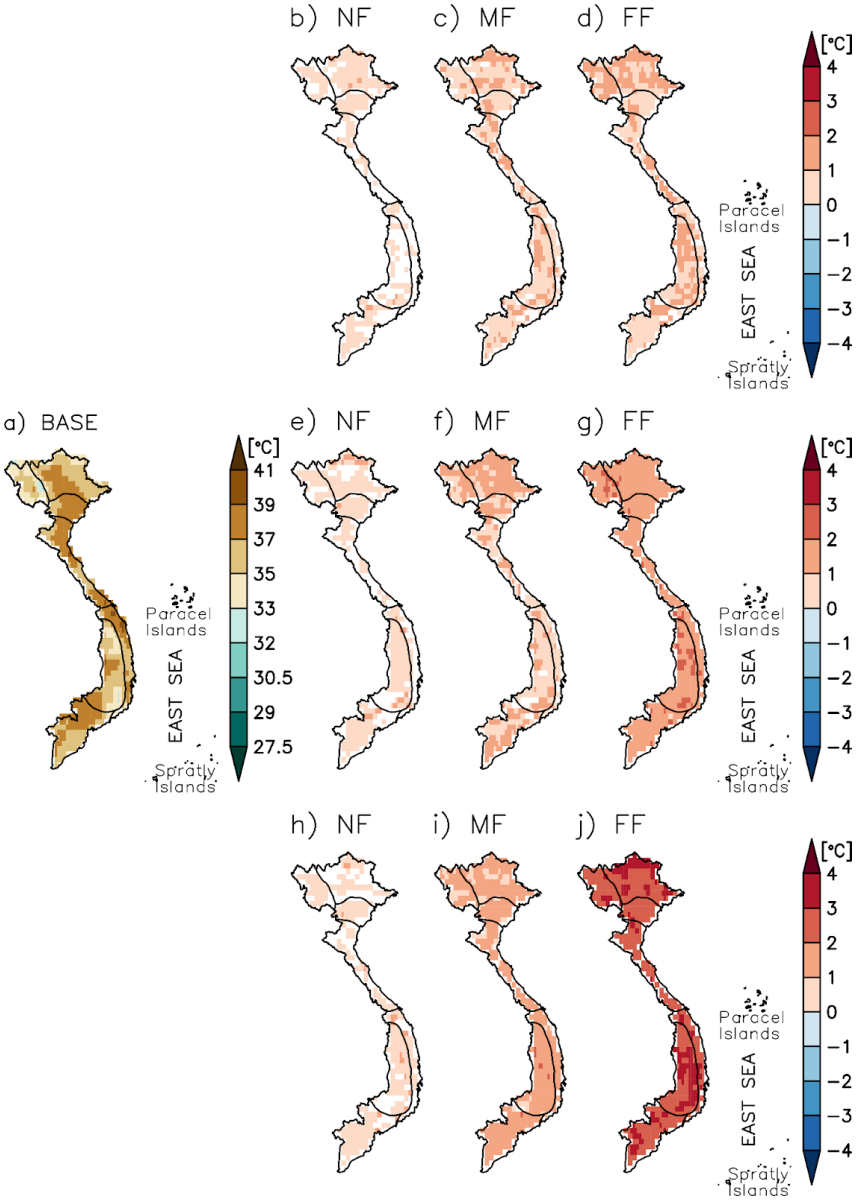

Source: Authors' own calculation. Original.

Figure 3. As in Figure 2 but for the annual number of days (Nx,3) when daily maximum WBGT (WBGTx) exceeds the Level 3 threshold (>32°C)

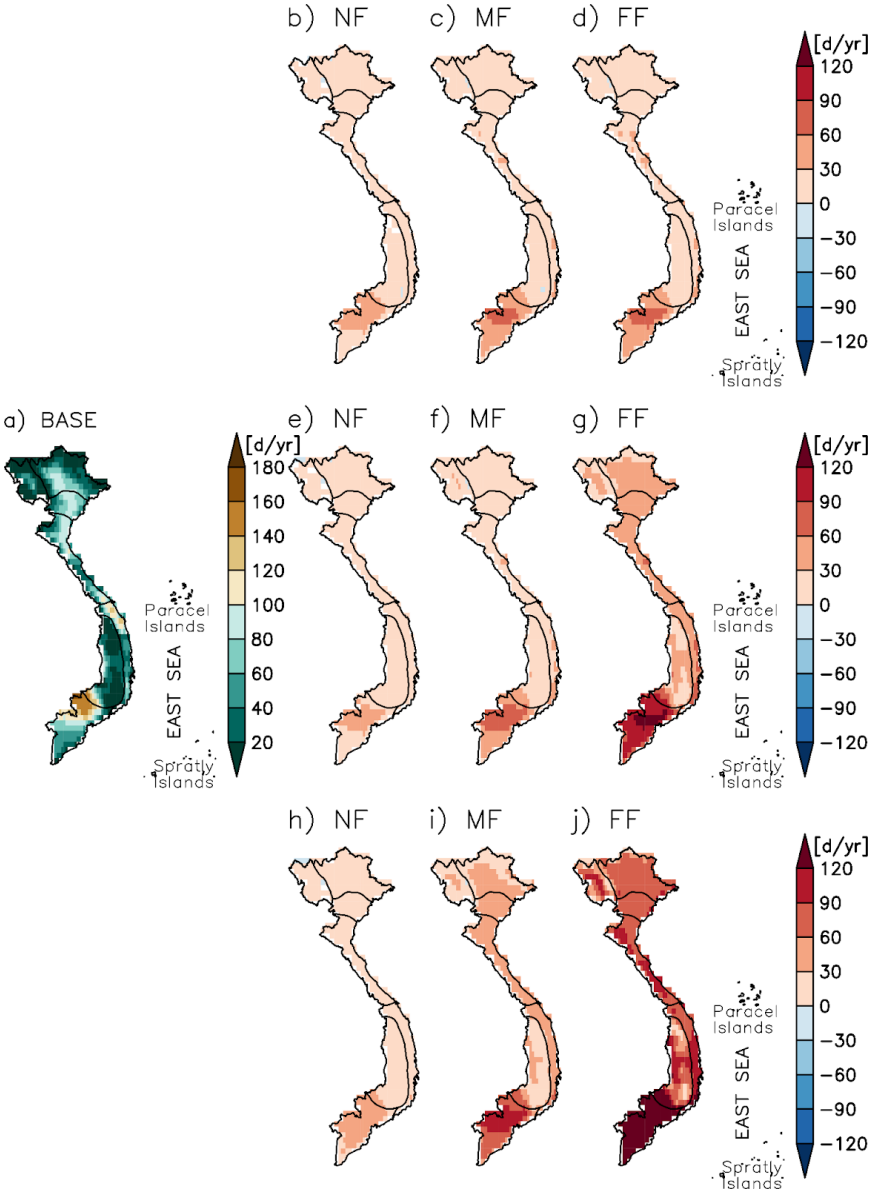

Source: Authors' own calculation. Original.

Similar patterns, but with even higher increases, are obtained for the annual maximum WBGTm (WBGTm,x) under SSP5-8.5 (Figure S3). In the far future, projected increases in WBGTm,x typically exceed 3oC and may approach 4oC across Vietnam, highlighting the severe impacts of high-emission scenarios. Likewise, under SSP5-8.5, the annual number of days (Nm,1) on which WBGTm exceeds the Level 1 (>29°C), which is almost zero in the current

climate, is projected to significantly increase in R2–R5 and R7 (Figure S4), exceeding 90 days per year in some areas by the far future. Similar results are projected at different GWLs, with increases scaling proportionally with GWL (Figure S5). Further, the increasing trends in WBGTm,x and Nm,1 exhibit consistent patterns aligned with their projected increases (Figures S6 and S7). Of particular concern are R3 (the Red River Delta) and R7 (the Mekong River Delta), the two most densely populated subregions in Vietnam, encompassing Hanoi, the capital, and Ho Chi Minh City, the largest city. In these areas, the urban heat island effect can further intensify heat stress, while their economic importance and high concentration of outdoor workers engaged in medium to heavy labor make them especially vulnerable. These findings indicate a substantial risk of future heat stress in these subregions, emphasizing the urgent need for effective mitigation and adaptation strategies. The following subsections will further investigate the detailed projections of heat stress at the subregional scale of Vietnam.

Figure 4. The spatial distribution of differences in annual maximum $WBGT_x$ ($WBGT_{x,x}$) between each GWL — (a) 1.5°C, (b) 2°C, (c) 3°C and (d) 4°C — and the baseline period (1995–2014) over Vietnam. (e), (f), (g), (h) are the same as (a), (b), (c), (d), respectively, but for the annual number of days ($N_{x,3}$) when $WBGT_x$ exceeds the Level 3 threshold (>32°C)

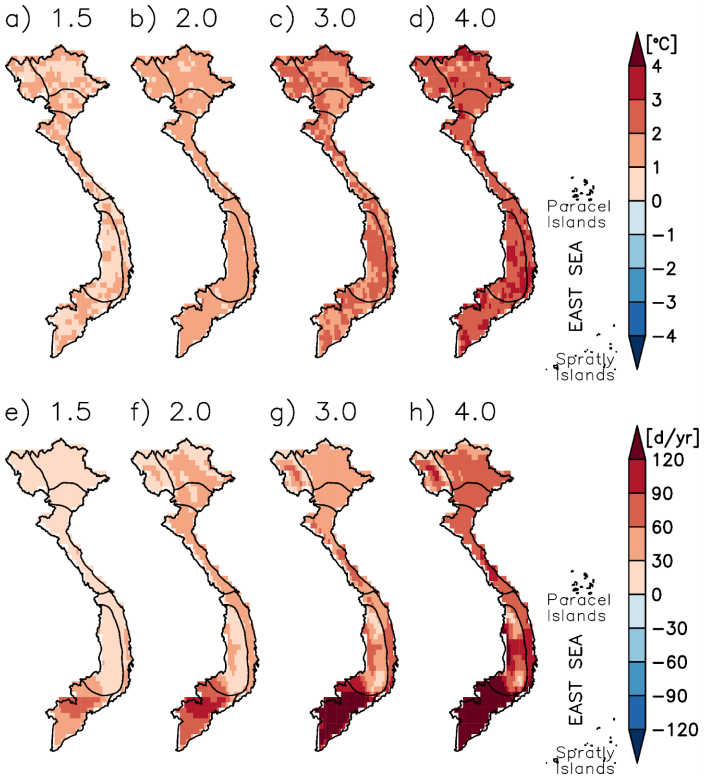

Source: Authors' own calculation. Original.

2.2. Detailed WBGT projections for seven subregions of Vietnam

The temporal evolution of area-averaged WBGTx,x for the seven sub-climatic regions of Vietnam is provided in Figure 5. Except for R1, WBGTx,x is already close to or approximately at the Level 4 (>37°C)during the baseline period, with R3 surpassing this threshold. Projections suggest that WBGTx,x will continue to increase under all scenarios, exceeding the Level 4 by the near to mid-future, except in R1. However, the intensity varies considerably by scenarios. Under SSP1-2.6, the positive aspect is that after exceeding the Level 4, the increasing rate in WBGTx,x slows down noticeably and tends to stabilize after the mid-future. Consequently, WBGTx,x in R1 remains well below the Level 4, while in other subregions, it mildly exceeds the threshold to the far future. However, projections are getting worse under "warmer" scenarios. Under SSP2-4.5, WBGTx,x increases slightly more than that under SSP1-2.6, with the differences generally less than 1°C. Specifically, in the far future, WBGTx,x in R3 is projected to reach 39°C, followed by R2 and R4–R7 at approximately 38°C, while R1 will approach 37°C. Finally, under the "warmest" SSP5-8.5, WBGTx,x in all subregions, including R1, are projected to exceed the Level 4, with the increase continuing throughout the century. By the far future, WBGTx,x under this pathway is expected to be about 3–3.5°C warmer than in the historical period across all subregions. R3 will experience the highest WBGTx,x of exceeding 40°C, followed by R2 and R4–R7 at around 39°C, while R1 reaches slightly above 37°C.

Figure 5. Temporal evolution of annual maximum WBGTx (WBGTx,x), averaged over seven subregions of Vietnam, under three Shared Socioeconomic Pathways: (green) SSP1-2.6, (blue) SSP2-4.5, and (red) SSP5-8.5

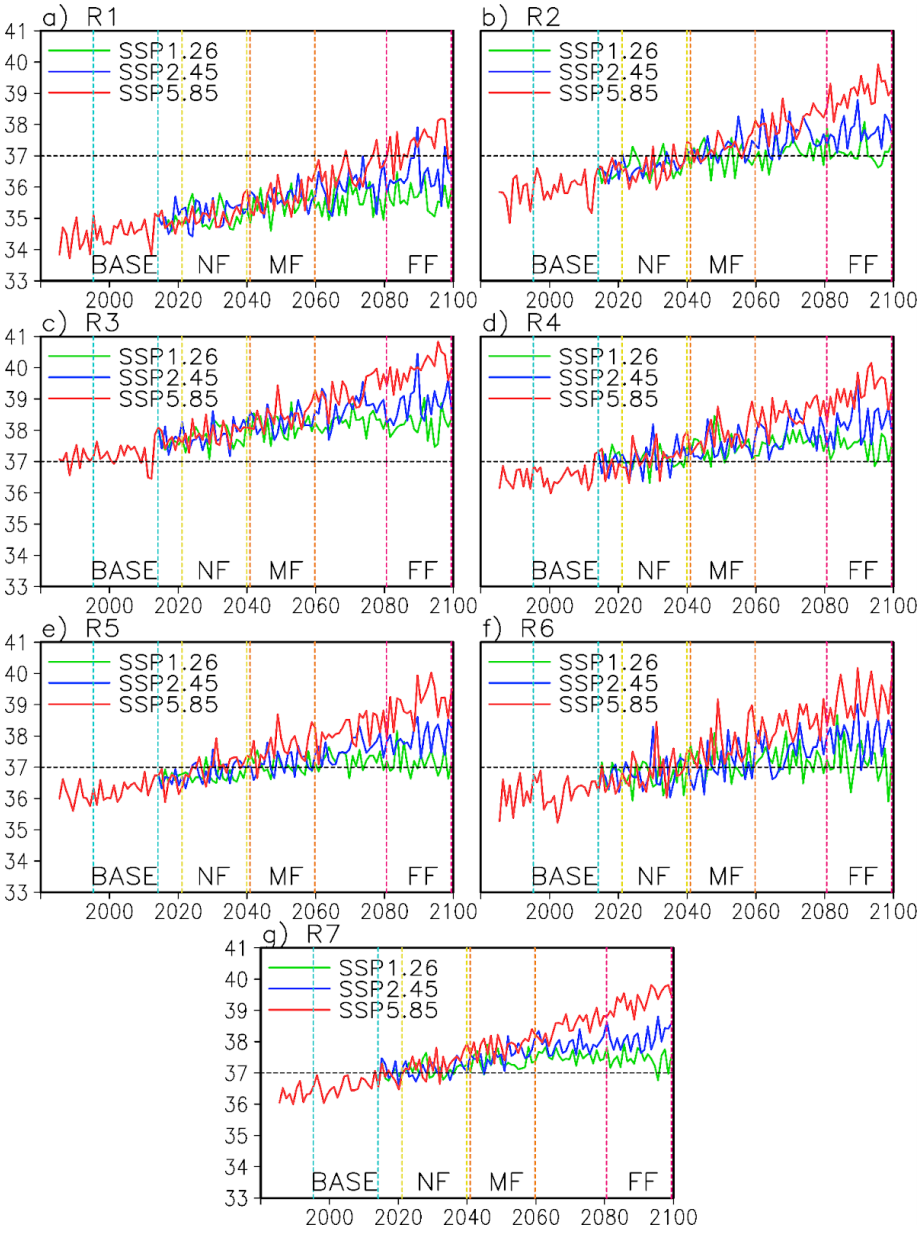

Source: Authors' own calculation. Original.

A particularly concerning aspect is the substantial increases in the annual number of the Level 3 (>32°C) exceedance days, Nx,3, especially by the end of this century under the "warmest" SSP5-8.5 scenario (Figure 6). During the historical period, Nx,3 was lowest in R1, with less than 10 dy/y. Values of 30–60 dy/y are observed in other subregions, except for R7, which recorded 60–90 dy/y. While increasing trends in Nx,3 are projected in all subregions, the magnitude of these increases varies significantly across both scenarios and subregions, with differences becoming more notable over time. By mid-century, most subregions show similar Nx,3 values across different pathways, except for R7, where the SSP5-8.5 already results in substantially higher $N_{x,3}$. In the latter half of this century, $N_{x,3}$ under SSP5-8.5 will increase much faster than those under other pathways. While increases in $N_{x,3}$ under SSP2-4.5 relative to SSP1-2.6 remain below 30 dy/y in R1–R6 and below 60 dy/y in R7, $N_{x,3}$ under SSP5-8.5 can potentially double those under SSP2-4.5 in the far future. For instance, while $N_{x,3}$ in R1 stays very low under both SSP1-2.6 and SSP2-4.5 through the century, it reaches more than 60 dy/y in the far future under SSP5-8.5. Similarly, $N_{x,3}$ in R2 is projected to be around 90 dy/y, while values in R3–R6 are expected to range between 120 and 150 dy/y by the end of the century under SSP5-8.5. A clear latitudinal gradient is also evident, with higher exceedance numbers projected in the southern subregions and decreasing values towards the north. Notably, projections for R7 indicate that $N_{x,3}$ could exceed 240–270 dy/y in the far future under SSP5-8.5, posing severe risks to human health and daily activities.

Figure 6. As in Figure 5 but for the number of days per year Nx,3 on which the Level 3 threshold of WBGTx is exceeded

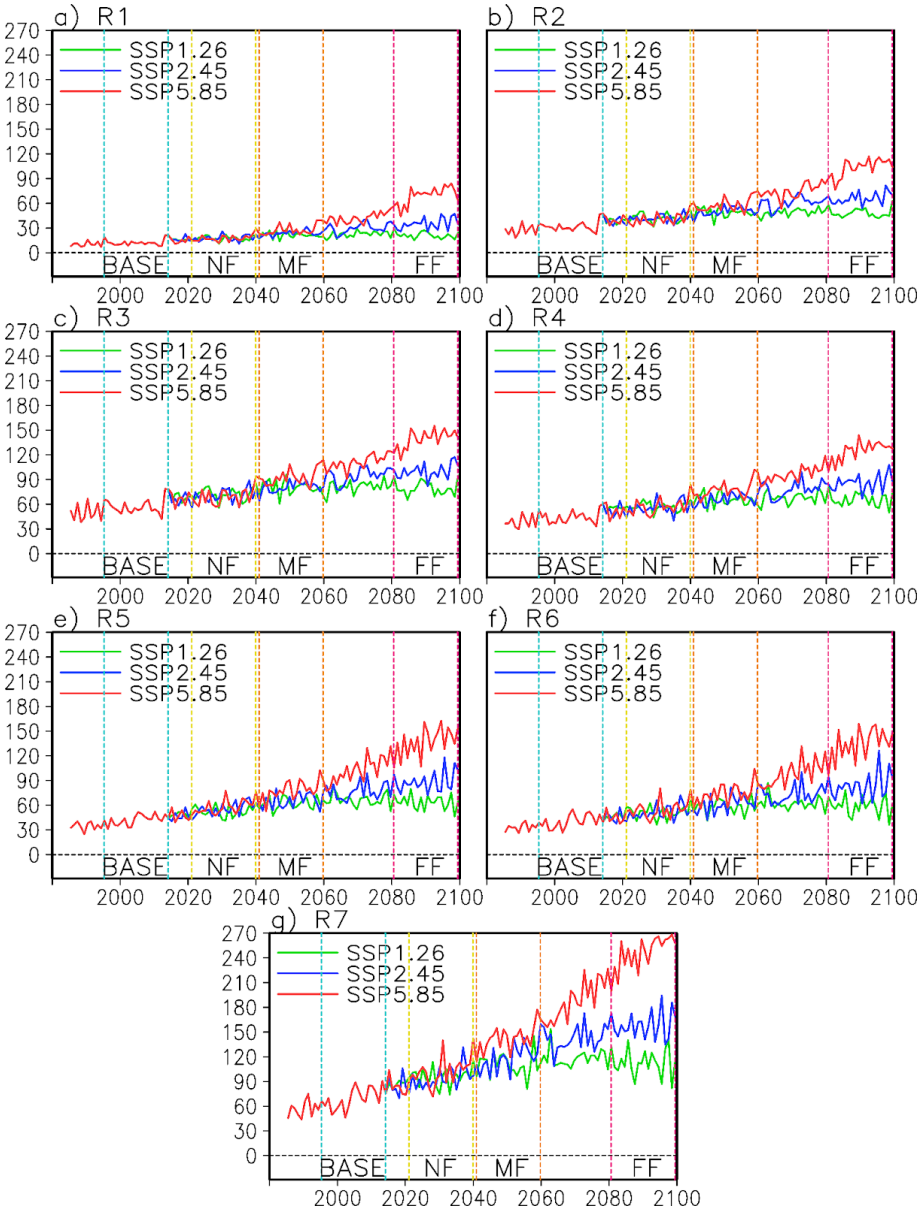

Source: Authors' own calculation. Original.

Figure 7 summarizes the increases in WBGTx characteristics, averaged over the seven subregions of Vietnam, at different GWLs relative to the baseline. As previously indicated, both WBGTx,x and Nx,3 increases exhibit a linear relationship with GWL. In detail, WBGTx,x, increases by approximately 1°C at GWL 1.5, 1–2°C at GWL 2°C, slightly exceeding 2°C at GWL 3°C, and approaching 3°C at GWL 4°C across all subregions (Figure 7a). For Nx,3, a latitudinal gradient is also found, with greater increases projected in the southern subregions. At GWLs 1.5°C, 2°C, 3°C, and 4°C, the increases of Nx,3 compared to the current climate remain below 30, 60, 90, and 120 d/yr, respectively, across most subregions, except for R7 (Figure 7b). In R7, the increase can exceed 60 and 90 d/yr at GWLs 1.5°C and 2°C, respectively, and reaches and surpasses 120 d/yr at GWLs of 3°C and higher.

Regarding WBGTm,x, the risks of future heat stress under SSP5-8.5 are also particularly pronounced in the Red River Delta (R3) and the Mekong River Delta (R7), where it exceeds the Level 1 (>29oC) as early as the mid-future (Figure S8). Significant increases in Nm,1 are also projected in these subregions, with values exceeding 70 dy/dy in R3 and 60 dy/y in R7 by the end of this century (Figure S9). Additionally, Nm,1 in R2, R4 and R7 reaches 30–40 dy/y under SSP5-8.5. On a more optimistic side, under SSP1-2.6 and SSP2-4.5, Nm,1 typically remains below 10 dy/y, except in R7, where it could reach 20 dy/y in the far future under SSP2-4.5. Once again, projected changes in subregional WBGTm characteristics at different GWLs exhibit increases that scale proportionally with GWL (Figure S10).

Figure 7. **(a) Differences in annual maximum WBGTx (WBGTx,x) averaged over the seven subregions of Vietnam between GWLs and the baseline period (1995–2014). (b) same as (a), but for the yearly number of days (Nx,3) when WBGTx exceeds the Level 3 threshold (>32°C).**

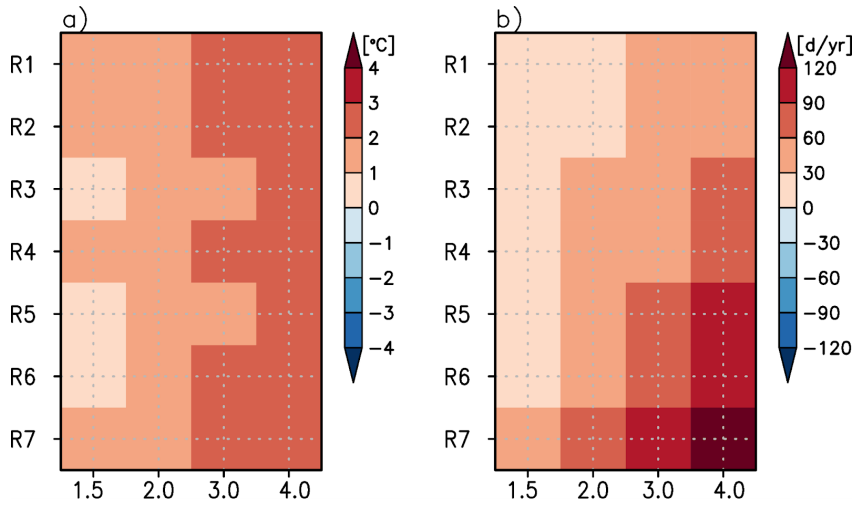

Source: Authors' own calculation. Original.

2.3. Comparison with sWBGT

As noted earlier, while simplified WBGT (sWBGT) has been widely used (Kjellstrom *et al.*, 2009; Willett and Sherwood 2012; Kakamu *et al.*, 2017; Lee and Min 2018; Zhu *et al.*, 2021), its accuracy has been questioned. To assess these biases, we compared analyses using sWBGT with our results as the reference standard. Detailed calculations of sWBGT are provided in Appendix A2. The analysis shows that sWBGT underestimates WBGTx,x in R1 and R6, which are mountainous regions, while overestimating it in eastern R2, R3, and R7, which are plains (Figure 8). It also leads to substantial overestimations of Nx,3 over most sub-regions, except in R1 and the high mountainous areas of R6 (Figure 9). For instance, for the baseline period, sWBGT overestimates Nx,3 by more than 120 d/yr in R7. These findings align with previous results (Kong and Huber 2022; Qiu *et al.*, 2024), which report that sWBGT tends to overestimate heat stress in hot-humid regions while underestimating extreme heat in dry regions. Similar biases are observed with WBGTm,x (Figure S11) and Nm,1 (Figure S12). These inaccuracies may result in misleading assessments, potentially triggering unnecessary alarms and negatively affecting adaptation strategies. A more comprehensive evaluation will be conducted in future research.

Figure 8. **Biases in annual maximum WBGTx (WBGTx,x) when using simplified WBGT (sWBGT) (sWBGT minus WBGT computed with the Liljegren's method) over Vietnam for (a) the baseline period and the (b), (e), (h) near future (NF; 2021–2040); (c), (f), (i) mid-future (MF; 2041–2060); and (d), (g), (j) far future (FF; 2081–2100) under three Shared Socioeconomic Pathways (top) SSP1-2.6, (middle) SSP2-4.5, and (bottom) SSP5-8.5. Only significant differences (p-value<0.05) are plotted.**

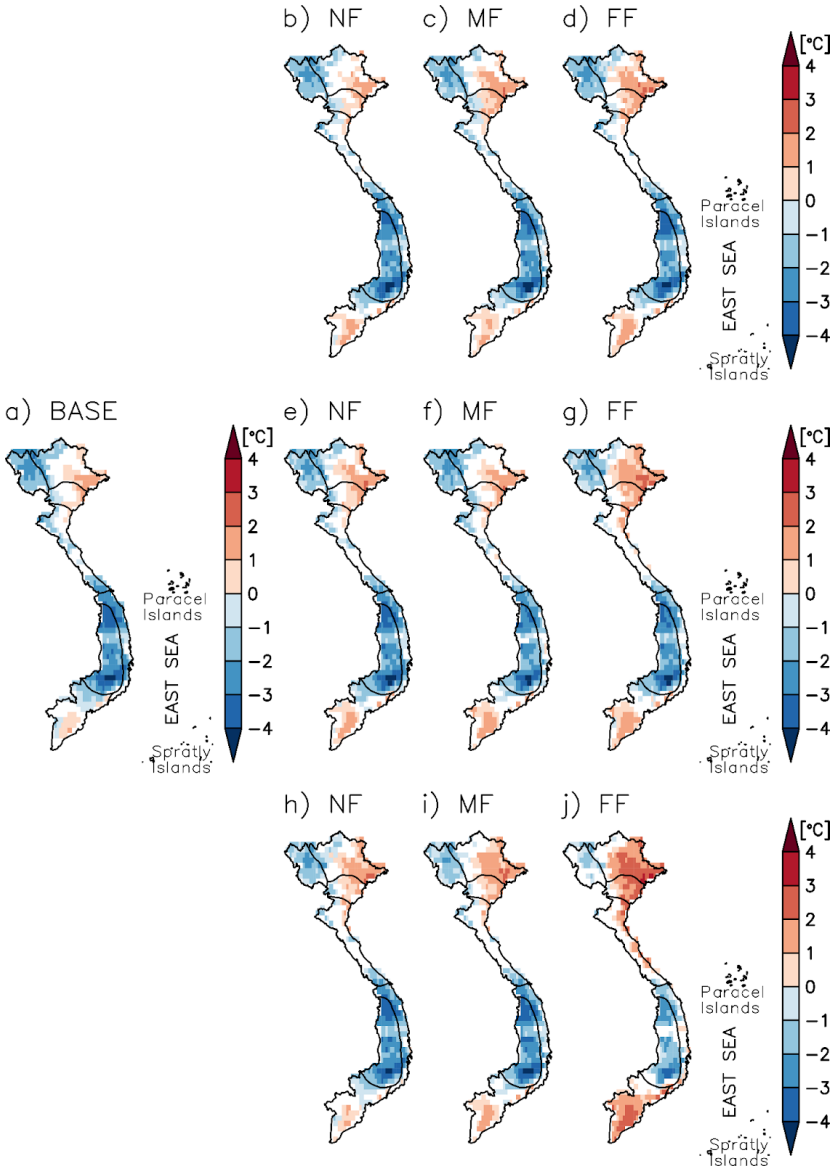

Source: Authors' own calculation. Original.

Figure 9. As in Figure 8 but for the annual number of days (Nx,3) on which daily maximum WBGT (WBGTx) exceeds the Level 3 threshold (>32°C)

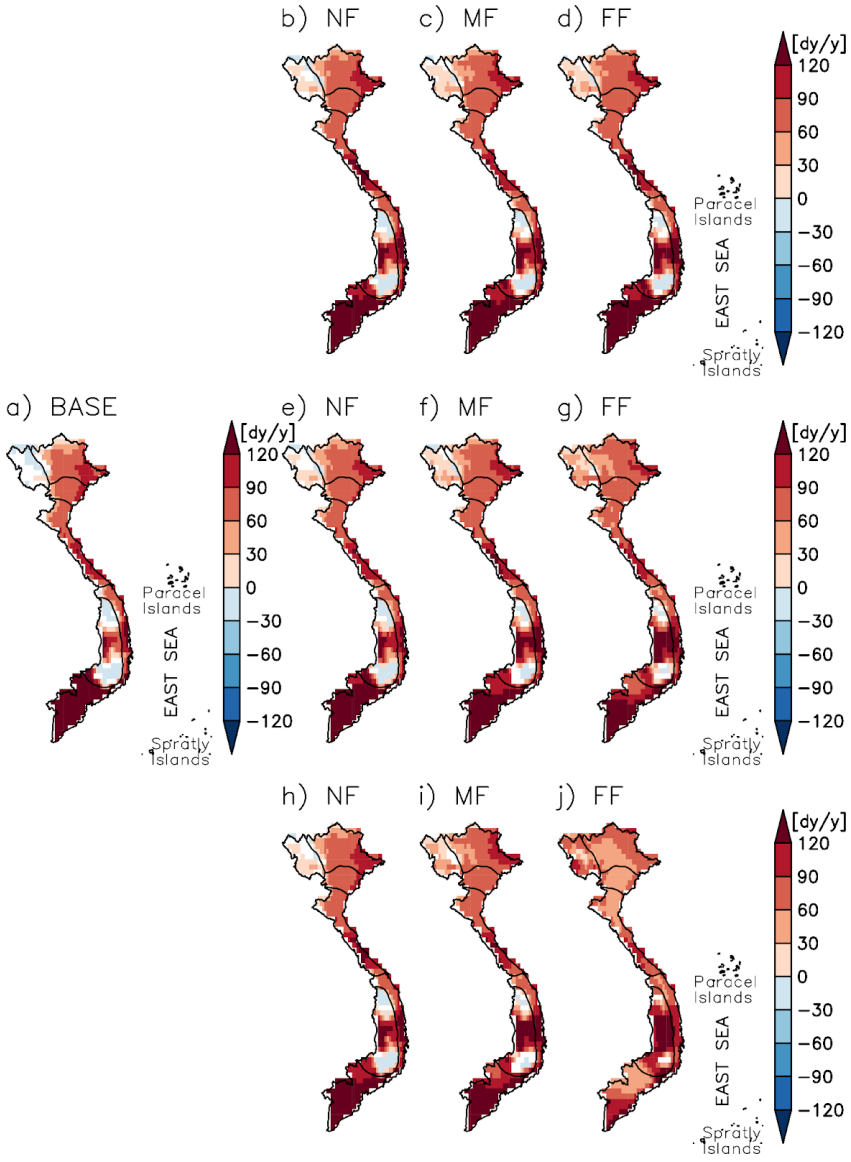

Source: Authors' own calculation. Original.

2.4. Discussion

Increases in WBGT will have significant implications for labor capacity, particularly in outdoor sectors such as agriculture and construction. A rise of just 1–2°C above the Level 1 threshold (>29°C)—or even lower for heavy and very heavy work (Appendix A.3)—can substantially reduce work capacity (Kjellstrom *et al.*, 2009). Historically, Level 3 (>32°C) exceedances have been relatively frequent in the plains but rare in mountainous regions.

However, these exceedances are projected to become more widespread, and all subregions of Vietnam are expected to experience unprecedented heat stress levels as early as mid-century across all scenarios and GWLs. This poses a significant threat to labor productivity and therefore could have severe socio-economic consequences. Nevertheless, existing adaptation strategies in Vietnam do not sufficiently address extreme heat risks, highlighting the urgent need for proactive planning and targeted adaptation measures. Hoang *et al.* (2022) for instance have highlighted the lack of consideration for heat hazards in current adaptation and development plan for the Mekong delta, while according to our results this region will be the most exposed to increasing heat hazards in future decades. Further, millions of people in urban centers such as Hanoi and Ho Chi Minh City will face intensified heat stress due to the urban heat island (UHI) effect, which is not accounted for in this study. Future research should integrate both climate change and UHI effects to provide a more comprehensive assessment of urban heat risks. Finally, it is important to acknowledge that universal thresholds may not fully capture regional and population-specific variations in adaptation and vulnerability to heat stress. Factors such as workload, age, gender, body composition, health, and socioeconomic status can influence human sensitivity to heat (McMichael *et al.*, 2006; Kjellstrom *et al.*, 2009). To account for these variations, different threshold levels have been proposed. For instance, Morabito *et al.*, (2019) incorporate height and weight to calculate metabolic rates and define risk thresholds. However, studies such as Schwingshackl *et al.* (2021) suggest that applying different thresholds can significantly impact exceedance rates. Therefore, further studies are requested to develop context-specific and regionally relevant thresholds for Vietnam.

Assessing the different types and efficiency of adaptation and mitigation strategies in the face of extreme heat is beyond the scope of this study. Measures could include for instance:

- Insuring access to sufficient amount of clean drinking water, especially for outdoor workers who may need more than 1L per hour (Morabito *et al.*, 2019).
- Providing protective clothing or personal protective equipment to workers and allowing sufficient short breaks (Hoa *et al.*, 2013).
- Shifting working hours. However, this strategy can significantly reduce labor productivity, as already observed when agricultural workers shift working hours to nighttime during heatwaves[1].

[1] https://www.weforum.org/stories/2020/06/vietnam-rice-farmers-global-warming-record-tempreatures/

- Developing warning system, ideally taking into account the metabolic rate (height, weight and activity level) (Morabito *et al.*, 2019). As highlighted in our study through the comparison of results obtained with sWBGT and WBGT according to Liljegren's method, heat stress indices must be carefully chosen to avoid under or over risk estimation.
- Insuring access to cooling centers for the most vulnerable population.
- Installing indoor cooling systems (fans and air conditioning). However, this strategy can increase greenhouse gases emissions, when electricity production relies on fossil fuels. In Vietnam, a high percentage of installed electric capacity still relies on coal (32.5%), gas (9,3%) and oil (1,9%). According to the Power Development Plan 8[2], Vietnamese electricity production should have phased out fossil fuel by 2050, however this trajectory remains very challenging in a context of rising energy demand.
- Improving thermal comfort indoor through adequate choice of building material and architecture (*e.g.* Latha *at al.*, 2015).
- Reducing the urban heat island effect, for instance through greening strategies (*e.g.* Trihamdani *et al.*, 2015; Scheuer *et al.*, 2024; Ramakreshnan & Aghamohammadi, 2024).
- Developping insurance-based mechanisms to avoid income reduction when labor intensity needs to be reduced to avoid heat stress.
- Consider increased heat hazards in power development plans. Indeed, increased electricity demand for cooling can put the power grid under pressure and drive power cuts, as was observed in Vietnam during the heat wave of May 2023[3].

Some of the above listed measures are short-term adaptations. But as stressed in another study for India (AchutaRao & Sagar, 2023), the magnitude of increase in heat hazards that could occur in future decades "*will require planning and adaptation measures beyond short-term disaster planning frameworks*".

[2] https://www.tresor.economie.gouv.fr/Articles/e7d47ae5-0801-44b9-a7f4-ba096740da61/files/fa191696-d8a7-443b-b513-7009e4b169e3

[3] https://www.lemonde.fr/en/asia-and-pacific/article/2023/06/08/vietnam-battles-record-heat-waves-and-power-cuts_6030467_153.html

3. Conclusions

Given the increasing emergence of heat stress in Vietnam, understanding its projected changes under global warming is crucial. The CORDEX-SEA initiative offers an opportunity to assess these future changes across seven subregions of Vietnam using prescribed radiative forcing scenarios and high-resolution outputs from the latest generation of climate models.

The findings indicate significant future increases in heat stress across Vietnam by the end of the century, especially under high-emission scenarios, and warmer GWLs. A critical concern is the substantial increase in the number of days exceeding impact-relevant heat stress thresholds, particularly pronounced in the Red River Delta and Mekong River Delta, the two most densely populated and agriculturally essential subregions of Vietnam. The emergence and intensity of heat stress are strongly correlated with the radiative forcing of the SSP scenarios and the GWLs, with higher forcing scenarios and warmer GWL leading to more severe heat stress and a greater frequency of exceedance days. The most severe impacts are projected exclusively under SSP5-8.5 as well as the GWLs 3°C and 4°C, underscoring the urgent need to limit future warming to mitigate the severe consequences of heat stress. However, as the world is currently on the path of ~2°C warming by mid-century and could reach 3°C by the end of the century (UNEP, 2024), Vietnam should prepare to face longer, hotter and more widespread heatwaves.

Note that this study analyzes the multi-model mean from only two downscaled CMIP6 GCMs, thus uncertainties remain in projecting heat stress in Vietnam. Further efforts should be made to enhance the credibility of these projections, such as incorporating more models. Future studies also benefit from considering multiple heat stress indices for comprehensive assessments (Shin *et al.*, 2022).

Bibliography

AchutaRao, K., & Sagar, A. D. (2023). Climate science to inform adaptation policy: Heat waves over India in the 1.5° C and 2°C warmer worlds. *Climatic Change*, 176(5), 64.

Barriopedro, D., Fischer, E. M., Luterbacher, J., Trigo, R. M., & García-Herrera, R. (2011). The hot summer of 2010: Redrawing the temperature record map of Europe. *Science*, 332(6026), 220–224.

Blazejczyk, K., Epstein, Y., Jendritzky, G., Staiger, H., & Tinz, B. (2012). Comparison of UTCI to selected thermal indices. *International Journal of Biometeorology*, 56(3), 515–535.

Bock, L., Lauer, A., Schlund, M., Barreiro, M., Bellouin, N., Jones, C., Meehl, G. A., Predoi, V., Roberts, M. J., & Eyring, V. (2020). Quantifying progress across different CMIP phases with the ESMValTool. *Journal of Geophysical Research: Atmospheres*, 125(21).

Buzan, J. R., Oleson, K., & Huber, M. (2015). Implementation and comparison of a suite of heat stress metrics within the Community Land Model version 4.5. *Geoscientific Model Development*, 8, 151–170.

Buzan, J. R., & Huber, M. (2020). Moist heat stress on a hotter earth. *Annual Review of Earth and Planetary Sciences*, 48(1), 623–655.

Cannon, A. J., Sobie, S. R., & Murdock, T. Q. (2015). Bias correction of GCM precipitation by quantile mapping: How well do methods preserve changes in quantiles and extremes? *Journal of Climate*, 28(17), 6938–6959.

Coppola, E., Stocchi, P., Pichelli, E., Torres Alavez, J. A., Glazer, R., Giuliani, G., Di Sante, F., Nogherotto, R., & Giorgi, F. (2021). Non-Hydrostatic RegCM4 (Regcm4-nh): Model description and case studies over multiple domains. *Geoscientific Model Development*, 14(12), 7705–7723.

Dang, T. N., Honda, Y., Van Do, D., Pham, A. L. T., Chu, C., Huang, C., & Phung, D. (2019). Effects of extreme temperatures on mortality and hospitalization in Ho Chi Minh City, Vietnam. *International Journal of Environmental Research and Public Health*, 16(3), 432.

de Freitas, C. R., & Grigorieva, E. A. (2017). A comparison and appraisal of a comprehensive range of human thermal climate indices. *International Journal of Biometeorology*, 61(3), 487–512.

Desmet, Q., & Ngo-Duc, T. (2022). A novel method for ranking CMIP6 global climate models over the Southeast Asian region. *International Journal of Climatology*, 42(1), 97–117.

Diffenbaugh, N. S., & Giorgi, F. (2012). Climate change hotspots in the CMIP5 global climate model ensemble. *Climatic Change*, 114(3), 813–822.

Dunne, J. P., Stouffer, R. J., & John, J. G. (2013). Reductions in labour capacity from heat stress under climate warming. *Nature Climate Change*, 3(6), 563–566.

Ebi, K. L., Vanos, J., Baldwin, J. W., Bell, J. E., Hondula, D. M., Errett, N. A., Hayes, K., Reid, C. E., Saha, S., Spector, J., & Berry, P. (2021). Extreme weather and climate change: Population health and health system implications. *Annual Review of Public Health*, 42(1), 293–315.

Eyring, V., Bony, S., Meehl, G. A., Senior, C. A., Stevens, B., Stouffer, R. J., & Taylor, K. E. (2016). Overview of the coupled model intercomparison project phase 6 (CMIP6) experimental design and organization. *Geoscientific Model Development*, 9(5), 1937–1958.

Gao, C., Kuklane, K., Östergren, P.-O., & Kjellstrom, T. (2019). Surveillance of work environment and heat stress assessment using meteorological data. *International Journal of Biometeorology*, 63(2), 195–196.

Grundstein, A., Williams, C., Phan, M., & Cooper, E. (2015). Regional heat safety thresholds for athletics in the contiguous United States. *Applied Geography*, 56, 55–60.

Hauser, M., Engelbrecht, F., & Fischer, E. M. (2022). Transient global warming levels for CMIP5 and CMIP6 (Version v0.3.0) [Computer software]. Zenodo. https://doi.org/10.5281/zenodo.7390473.

Hausfather, Z., Marvel, K., Schmidt, G. A., Nielsen-Gammon, J. W., & Zelinka, M. (2022). Climate simulations: recognize the 'hot model'problem. *Nature*, *605*(7908), 26-29.

Hersbach, H., Bell, B., Berrisford, P., Hirahara, S., Horányi, A., Muñoz-Sabater, J., Nicolas, J., Peubey, C., Radu, R., Schepers, D., Simmons, A., Soci, C., Abdalla, S., Abellan, X., Balsamo, G., Bechtold, P., Biavati, G., Bidlot, J., Bonavita, M., ... Thépaut, J. (2020). The ERA5 global reanalysis. *Quarterly Journal of the Royal Meteorological Society*, 146(730), 1999–2049.

Hoa, D.T.M., Nguyet, D.N., Phuong, N.H., Phuong, D.T., Nga, V.T., Few, R. & Winkels, A. (2013). Heat stress and adaptive capacity of low-income outdoor workers and their families in the city of Da Nang, Vietnam. *Asian Cities Climate Resilience, Working Paper Series*, 3.

Hoang, T. L. T., Dao, H. N., Cu, P. T., Tran, V. T. T., Tong, T. P., Hoang, S. T., Vuong, V. V., & Nguyen, T. N. (2022). Assessing heat index changes in the context of climate change: A case study of Hanoi (Vietnam). *Frontiers in Earth Science*, 10, 897601.

Hoang, V.T.M., Huynh, T.P.L., Tamas, P., Minderhoud, P., Woillez, M.-N., Espagne, E. & Umans, L. (2022). Adaptation strategies in the Delta: are they consistent with current and future changes?
In: The Mekong Delta Emergency, Climate and Environmental Adaptation Strategies to 2050. Final Report GEMMES Viet Nam Project. Woillez, M.-N. & Espagne, E. (Ed.).

Im, E.-S., Pal, J. S., & Eltahir, E. A. B. (2017). Deadly heat waves projected in the densely populated agricultural regions of South Asia. Science Advances, 3(8), e1603322.

Intergovernmental Panel on Climate Change (IPCC) (2021). Climate change 2021 – the physical science basis: Working group I contribution to the sixth assessment report of the intergovernmental panel on climate change. Cambridge University Press. https://doi.org/10.1017/9781009157896

ISO (2017). Ergonomics of the thermal environment—Assessment of heat stress using the WBGT (wet bulb globe temperature) index (International Standard). *International Organization for Standardization*.

Jacobs, C., Singh, T., Gorti, G., Iftikhar, U., Saeed, S., Syed, A., Abbas, F., Ahmad, B., Bhadwal, S., & Siderius, C. (2019). Patterns of outdoor exposure to heat in three South Asian cities. *Science of The Total Environment*, 674, 264–278.

Kakamu, T., Wada, K., Smith, D. R., Endo, S., & Fukushima, T. (2017). Preventing heat illness in the anticipated hot climate of the Tokyo 2020 Summer Olympic Games. *Environmental Health and Preventive Medicine*, 22(1), 68.

Kjellstrom, T., Briggs, D., Freyberg, C., Lemke, B., Otto, M., & Hyatt, O. (2016). Heat, human performance, and occupational health: A key issue for the assessment of global climate change impacts. *Annual Review of Public Health*, 37(1), 97–112.

Kjellstrom, T., Freyberg, C., Lemke, B., Otto, M., & Briggs, D. (2018). Estimating population heat exposure and impacts on working people in conjunction with climate change. *International Journal of Biometeorology*, 62(3), 291–306.

Kjellstrom, T., Holmer, I., & Lemke, B. (2009). Workplace heat stress, health and productivity – an increasing challenge for low and middle-income countries during climate change. *Global Health Action*, 2(1), 2047.

Kong, Q., & Huber, M. (2022). Explicit calculations of wet-bulb globe temperature compared with approximations and why it matters for labor productivity. *Earth's Future*, 10(3), e2021EF002334.

Latha, P. K., Darshana, Y., & Venugopal, V. (2015). Role of building material in thermal comfort in tropical climates–A review. *Journal of Building Engineering*, *3*, 104-113.

Lee, S.-M., & Min, S.-K. (2018). Heat stress changes over East Asia under 1. 5° and 2. 0°C global warming targets. *Journal of Climate*, 31(7), 2819–2831.

Lemke, B., & Kjellstrom, T. (2012). Calculating workplace WBGT from meteorological data: A tool for climate change assessment. *Industrial Health*, 50(4), 267–278.

Li, D., Yuan, J., & Kopp, R. E. (2020). Escalating global exposure to compound heat-humidity extremes with warming. *Environmental Research Letters*, 15(6), 064003.

Liljegren, J. C., Carhart, R. A., Lawday, P., Tschopp, S., & Sharp, R. (2008). Modeling the wet bulb globe temperature using standard meteorological measurements. *Journal of Occupational and Environmental Hygiene*, 5(10), 645–655.

Maia-Silva, D., Kumar, R., & Nateghi, R. (2020). The critical role of humidity in modeling summer electricity demand across the United States. *Nature Communications*, 11(1), 1686.

Maraun, D. (2016). Bias correcting climate change simulations—A critical review. *Current Climate Change Reports*, 2(4), 211–220.

McMichael, A. J., Woodruff, R. E., & Hales, S. (2006). Climate change and human health: Present and future risks. *The Lancet*, 367(9513), 859–869.

Morabito, M., Messeri, A., Noti, P., Casanueva, A., Crisci, A., Kotlarski, S., Orlandini, S., Schwierz, C., Spirig, C., Kingma, B. R. M., Flouris, A. D., & Nybo, L. (2019). An occupational heat–health warning system for Europe: The heat-shield platform. *International Journal of Environmental Research and Public Health*, 16(16), 2890.

NASA Shuttle Radar Topography Mission (SRTM) (2013). Shuttle Radar Topography Mission (SRTM) Global. Distributed by OpenTopography. https://doi.org/10.5069/G9445JDF. Accessed: 2025-03-05

Nguyen D. N. and Nguyen T. H. (2004). Climate and climatic resources of Vietnam. Agricultural Publisher, Hanoï (in Vietnamese).

Ngo-Duc, T., Nguyen-Duy, T., Desmet, Q., Trinh-Tuan, L., Ramu, L., Cruz, F., Dado, J. M., Chung, J. X., Phan-Van, T., Pham-Thanh, H., Truong-Ba, K., Tangang, F. T., Juneng, L., Santisirisomboon, J., Srisawadwong, R., Permana, D., Linarka, U. A., & Gunawan, D. (2024). Performance ranking of multiple CORDEX-SEA sensitivity experiments: Towards an optimum choice of physical schemes for RegCM over Southeast Asia. *Climate Dynamics*, 62(9), 8659–8673.

O'Neill, B. C., Kriegler, E., Ebi, K. L., Kemp-Benedict, E., Riahi, K., Rothman, D. S., van Ruijven, B. J., van Vuuren, D. P., Birkmann, J., Kok, K., Levy, M., & Solecki, W. (2017). The roads ahead: Narratives for shared socioeconomic pathways describing world futures in the 21st century. *Global Environmental Change*, 42, 169–180.

Orlov, A., Sillmann, J., Aunan, K., Kjellstrom, T., & Aaheim, A. (2020). Economic costs of heat-induced reductions in worker productivity due to global warming. *Global Environmental Change*, 63, 102087.

Phung, D., Chu, C., Rutherford, S., Nguyen, H. L. T., Do, C. M., & Huang, C. (2017). Heatwave and risk of hospitalization: A multi-province study in Vietnam. *Environmental Pollution*, 220, 597–607.

Qiu, L., Zhu, Z., Zhou, Z., Im, E.-S., Min, S.-K., Kim, Y.-H., Kim, Y., Cha, D.-H., Ahn, J.-B., & Byun, Y.-H. (2024). Amplification of the discrepancy between simplified and physics-based wet-bulb globe temperatures in a warmer climate. *Weather and Climate Extremes*, 44, 100677.

Ramakreshnan, L., & Aghamohammadi, N. (2024). The application of nature-based solutions for urban heat island mitigation in Asia: progress, challenges, and recommendations. *Current environmental health reports*, *11*(1), 4-17.

Schleussner, C.-F., Donges, J. F., Donner, R. V., & Schellnhuber, H. J. (2016). Armed-conflict risks enhanced by climate-related disasters in ethnically fractionalized countries. *Proceedings of the National Academy of Sciences*, 113(33), 9216–9221.

Schwingshackl, C., Sillmann, J., Vicedo-Cabrera, A. M., Sandstad, M., & Aunan, K. (2021). Heat stress indicators in CMIP6: Estimating future trends and exceedances of impact-relevant thresholds. *Earth's Future*, 9(3), e2020EF001885.

Shen, B., Hu, X., & Wu, H. (2020). Impacts of climate variations on crime rates in Beijing, China. *Science of The Total Environment*, 725, 138190.

Sherwood, S. C., & Huber, M. (2010). An adaptability limit to climate change due to heat stress. Proceedings of the National *Academy of Sciences*, 107(21), 9552–9555.

Scheuer, S., Sumfleth, L., Nguyen, L. D. H., Vo, Y., Hoang, T. B. M., & Jache, J. (2024). A Systematic Assessment of Greening Interventions for Developing Best Practices for Urban Heat Mitigation—The Case of Hué, Vietnam. *Urban Science*, *8*(2), 67.

Shin, J.-Y., Kang, M., & Kim, K. R. (2022). Outdoor thermal stress changes in South Korea: Increasing inter-annual variability induced by different trends of heat and cold stresses. *Science of The Total Environment*, 805, 150132.

Tangang, F., Chung, J. X., Juneng, L., Supari, Salimun, E., Ngai, S. T., Jamaluddin, A. F., Mohd, M. S. F., Cruz, F., Narisma, G., Santisirisomboon, J., Ngo-Duc, T., Van Tan, P., Singhruck, P., Gunawan, D., Aldrian, E., Sopaheluwakan, A., Grigory, N., Remedio, A. R. C., ... Kumar, P. (2020). Projected future changes in rainfall in Southeast Asia based on CORDEX–SEA multi-model simulations. *Climate Dynamics*, 55(5), 1247–1267.

Trihamdani, A. R., Lee, H. S., Kubota, T., & Phuong, T. T. T. (2015). Configuration of green spaces for urban heat island mitigation and future building energy conservation in Hanoi Master Plan 2030. *Buildings*, *5*(3), 933-947.

United Nations Environment Programme (2024). Executive summary. In Emissions Gap Report 2024: No more hot air … please! With a massive gap between rhetoric and reality, countries draft new climate commitments. Nairobi.

UNFCCC (2007). Climate change: impacts, vulnerabilities and adaptation in developing countries. *United Nations Framework Convention on Climate Change*, Climate Change Secretariat (UNFCCC), Bonn

Vu, N., & Ngo-Duc, T. (2024). Spatial distribution and trends of heat stress in Vietnam. *Environment and Natural Resources Journal*, 22(2), 1–12.

Willett, K. M., & Sherwood, S. (2012). Exceedance of heat index thresholds for 15 regions under a warming climate using the wet-bulb globe temperature. *International Journal of Climatology*, 32(2), 161–177.

Yaglou, C. P., & Minard, D. (1957). Control of heat casualties at military training centers, AMA Arch Ind Health, 16(4), 302-16.

Zhao, Y., Ducharne, A., Sultan, B., Braconnot, P., & Vautard, R. (2015). Estimating heat stress from climate-based indicators: Present-day biases and future spreads in the CMIP5 global climate model ensemble. Environmental Research Letters, 10(8), 084013.

Zhu, J., Wang, S., Zhang, B., & Wang, D. (2021). Adapting to changing labor productivity as a result of intensified heat stress in a changing climate. *GeoHealth*, 5(4), e2020GH000313.

Zscheischler, J., Fischer, E. M., & Lange, S. (2019). The effect of univariate bias adjustment on multivariate hazard estimates. *Earth System Dynamics*, 10(1), 31–43.

Appendix

A.1. Descriptions and equations of Liljegren's model

Liljegren's model provides a more accurate and robust method for estimating WBGT compared to simpler approximations. It performs energy budget analyses on both natural wet-bulb and black globe sensors, which boil down to two separate equations for T_w (Equation S1) and T_g (Equation S3) (Liljegren *et al.*, 2008) that need to be solved by iteration:

$$T_W = T_a - \frac{\Delta H}{C_p}\frac{M_{H20}}{M_{Air}}\left(\frac{Pr}{Sc}\right)^{0.56}\left(\frac{e_w - e_a}{P - e_a}\right) + \frac{\Delta F_{net}}{Ah} \quad \text{(S1)}$$

where ΔH is heat of vaporization; cp is the specific heat of dry air at constant pressure; M_{H20} and M_{air} are, respectively, the molecular weight of dry air and water vapour; *Pr* and *Sc* are , respectively, Prandtl and Schmidt number; *P* and e_w are, respectively, surface pressure and vapor pressure at the surface of the wick; e_a is ambient vapor pressure; *h* is a convective heat transfer coefficient, which is a function of air temperature, pressure, wind speed, and the shape of T_w or T_g sensors; and ΔF_{net} refers to net radiative gain by the wick:

$$\begin{aligned}\Delta F_{net} = \tfrac{1}{2}\pi DL\epsilon_w\left(L_{down} + L_{up}\right) - \pi DL\sigma\epsilon_w T_w^4 + \left(\pi DL + \tfrac{\pi D^2}{4}\right)\left(1 - \alpha_w\right)\left(1 - f_{dir}\right)S_{down} \\ + \left(DLsin\theta + \tfrac{\pi D^2}{4}cos\theta\right)\left(1 - \alpha_w\right)f_{dir}\tfrac{S_{down}}{cos\theta} + \pi DL\left(1 - \alpha_w\right)S_{up}\end{aligned} \quad \text{(S2)}$$

where *D* and *L*, respectively, is diameter and length of wick; θ is solar zenith angle; S_{down}, S_{up}, L_{down}, and L_{up} denote surface downward and upwelling solar and long-wave radiation, respectively; fdir represents the fraction of the total horizontal solar irradiance due to the direct beam of the sun; σ is the Stefan-Boltzmann constant; ϵ_w and α_w are, respectively, the emissivity and albedo of the wick. The energy budget analysis on the black globe sensor leads to the equation below for T_g:

$$T_g^4 = \frac{L_{down} + L_{up}}{2\pi} - \frac{h\left(T_g - T_a\right)}{\epsilon_g\sigma} + \frac{S_{down}\left(1-\alpha_g\right)}{\epsilon_g\sigma}\left(1 - f_{dir} + \frac{f_{dir}}{2cos\theta}\right) + \frac{\left(1-\alpha_g\right)}{2\epsilon_g\sigma}S_{up} \quad \text{(S3)}$$

where ϵ_g and α_g represent the emissivity and albedo of the globe, respectively. In Liljegren's original formulation, the radiation components, S_{up}, L_{down} and L_{up}, were approximated as:

$$L_{down} = \sigma\epsilon_a T_a^4 \quad \text{(S4)}$$

$$L_{up} = \sigma\epsilon_{sfc} T_{sfc}^4 = \sigma T_a^4 \quad \text{(S5)}$$

$$S_{up} = \epsilon_{sfc} S_{down} \quad \text{(S6)}$$

where ϵ_a is the emissivity of the air; T_{sfc}, ϵ_{sfc}, and α_{sfc} are, respectively, the temperature, emissivity, and albedo of the surface.

Air temperature, humidity, wind speed, and surface downward solar radiation are required as inputs for solving T_w and T_g using Liljegren's model. For details on the calculation procedure, refer to Liljegren *et al.* (2008).

A.2. Simplified approximation of WBGT (sWBGT)

sWBGT (Anon 1984) is applied to approximate outdoor WBGT as a function of T_a and *RH* (Equation S7), assuming constant moderate solar radiation and relatively low wind speed.

$$sWBGT = 0.567T_a + 0.393e + 3.94 \quad \text{(S7)}$$

where *e* is the vapor pressure (hPa) calculated as

$$e = \left(\frac{RH}{100}\right) * 6.105 * exp\left(\frac{17.62T_d}{243.12+T_d}\right) \quad \text{(S1)}$$

where T_d denotes dew point temperature

References

Anon (1984). Prevention of thermal injuries during distance running. *Position stand, Medical Journal of Australia*, 141 876–9 Online: https://onlinelibrary.wiley.com/doi/abs/10.5694/j.1326-5377.1984.tb132981.x

Liljegren, J. C., Carhart, R. A., Lawday, P., Tschopp, S., & Sharp, R. (2008). Modeling the wet bulb globe temperature using standard meteorological measurements. *Journal of occupational and environmental hygiene*, *5*(10), 645-655.

A.3. Recommended maximum WBGT exposure levels

Table A.1. Recommended maximum WBGT exposure levels (°C) at different work intensities and rest/work ratios for an average acclimatised worker wearing light clothing. Light, medium, heavy and very heavy work correspond to metabolic rates of about 100,200,300,400 and 500 Watts respectively. If the worker uses heavier clothing or protective clothing, these values need to be reduced.

Work intensity	Light work	Medium work	Heavy work	Very heavy work
	WBGT(°C)	WBGT(°C)	WBGT(°C)	WBGT(°C)
Continuous work	31	28	27	25.5
25% rest/hour	31.5	29	27.5	26.5
50% rest/hour	32	30.5	29.5	28
75% rest/hour	32.5	32	31.5	31
No work at all	39	37	36	34

Source: Kjellstrom *et al.* (2009).

A.4. Suporting Figures

Figure S1. **Trends (°C/decade) in annual maximum WBGTx (WBGTx,x) over Vietnam during the entire studied period (1985–2100) under three Shared Socioeconomic Pathways (a) SSP1-2.6, (b) SSP2-4.5, and (c) SSP5-8.5. Only significant trends (p-value<0.05) are plotted.**

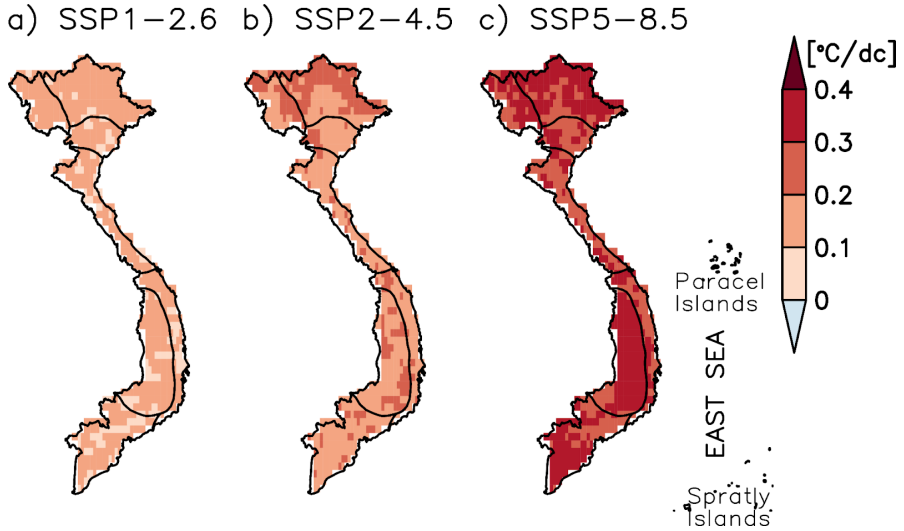

Figure S2. **Trends (day/decade) in the annual number of days (Nx,3) on which daily maximum WBGT (WBGTx) exceeds the Level 3 threshold (>32°C) during the study period (1985–2100) under three Shared Socioeconomic Pathways (a) SSP1-2.6, (b) SSP2-4.5, and (c) SSP5-8.5. Only significant trends (p-value<0.05) are plotted.**

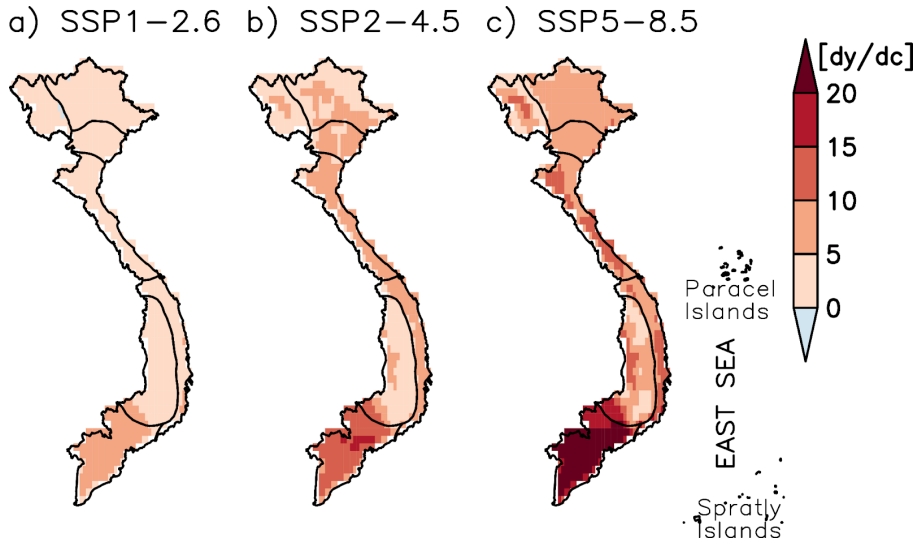

Figure S3. **(a) The spatial distribution of climatological annual maximum WBGTm (WBGTm,x) over Vietnam during the baseline period (1995–2014) and its projected changes for the (b), (e), (h) near future (NF; 2021–2040); (c), (f), (i) mid-future (MF; 2041–2060); and (d), (g), (j) far future (FF; 2081–2100) under three Shared Socioeconomic Pathways (top) SSP1-2.6, (middle) SSP2-4.5, and (bottom) SSP5-8.5. Only significant differences (p-value<0.05) are plotted.**

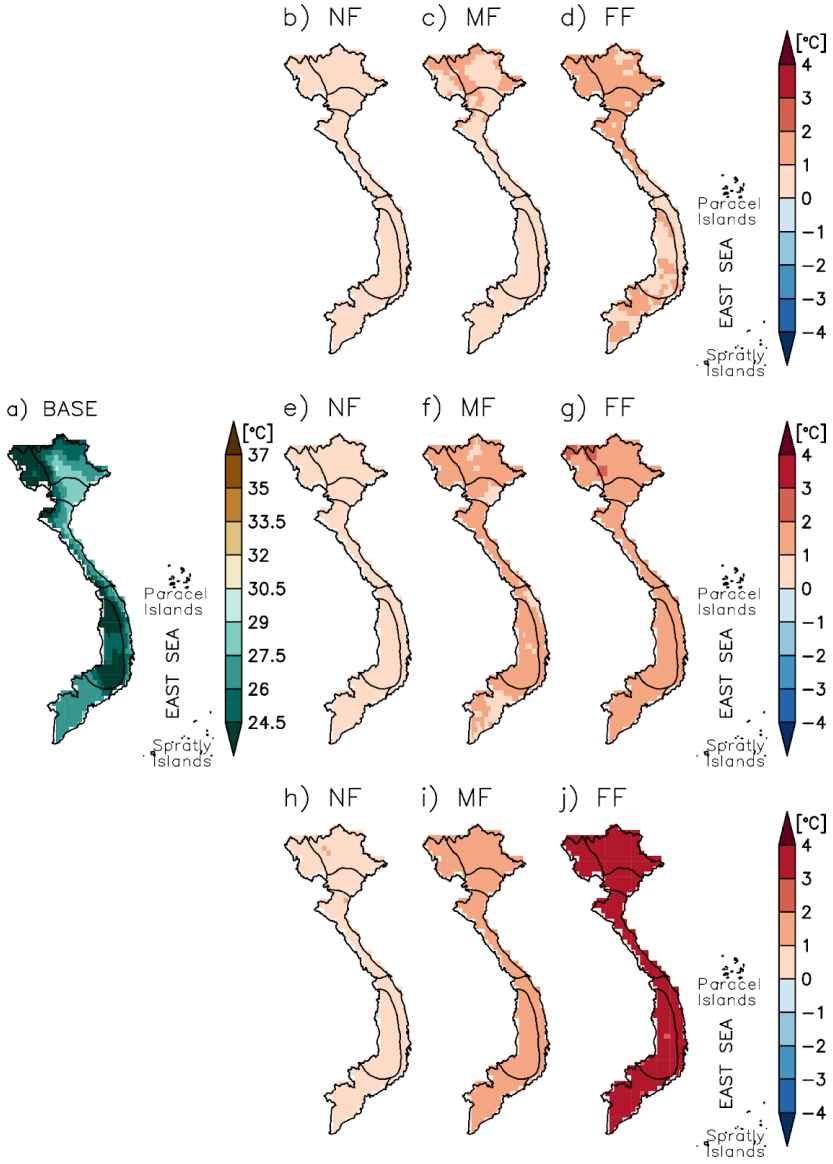

Figure S4. As in Figure S3 but for the annual number of days (Nm,1) when daily minimum WBGT (WBGTm) exceeds the Level 1 threshold (>29°C)

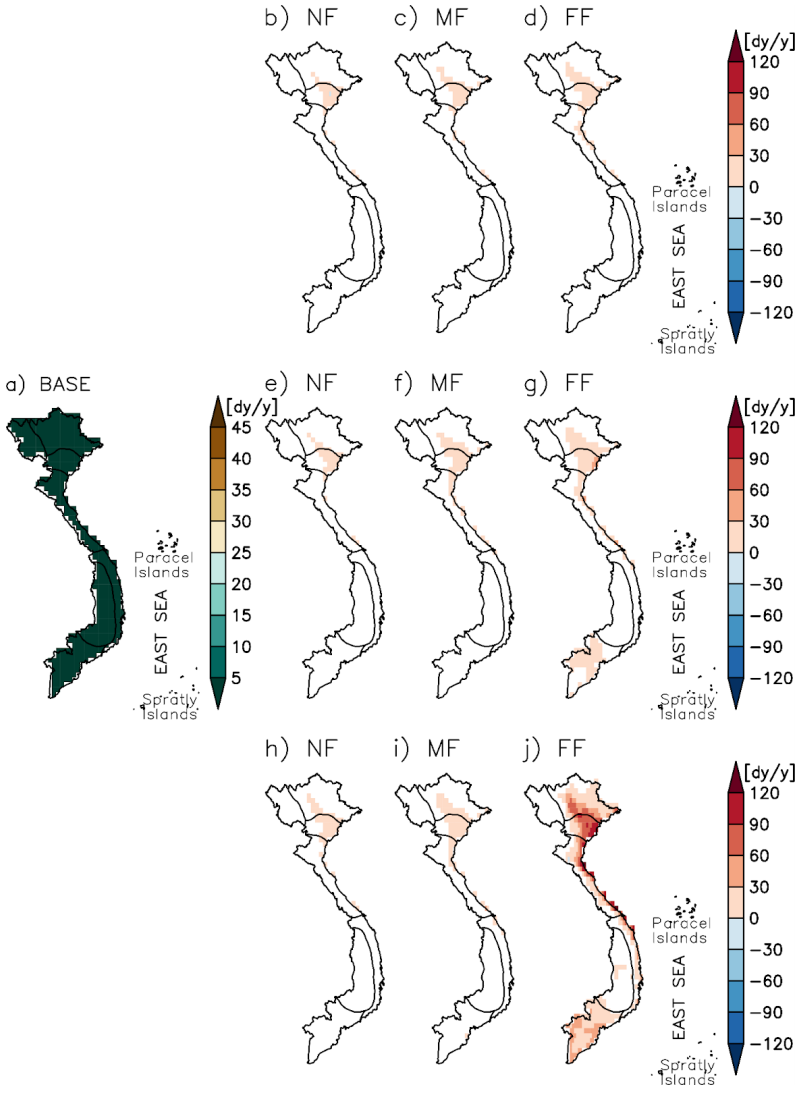

Figure S5. **The spatial distribution of differences in annual maximum WBGTm (WBGTm,x) between each GWL — (a) 1.5°C, (b) 2°C, (c) 3°C and (d) 4°C — and the baseline period (1995–2014) over Vietnam. (e), (f), (g), (h) are the same as (a), (b), (c), (d), respectively, but for the annual number of days (Nm,1) when WBGTm exceeds the Level 1 threshold (>29oC).**

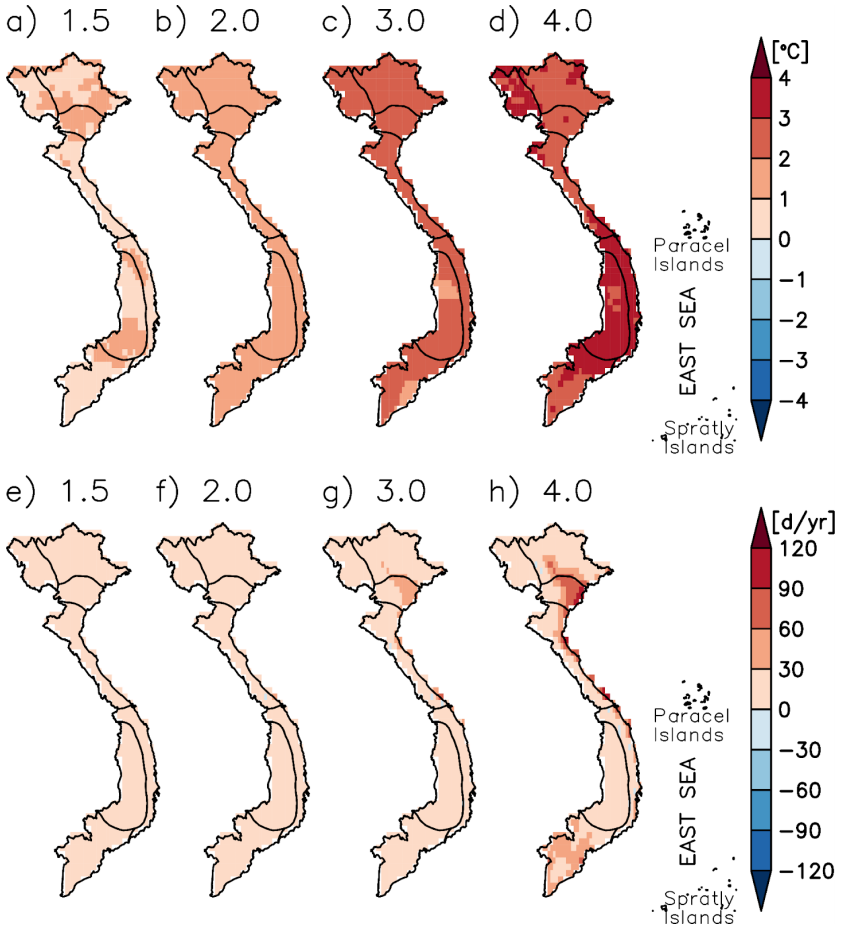

Figure S6. **Trends (°C/decade) in annual maximum WBGTm (WBGTm,x) over Vietnam during the entire studied period (1985–2100) under three Shared Socioeconomic Pathways (a) SSP1-2.6 , (b) SSP2-4.5, and (c) SSP5-8.5 (bottom). Only significant trends (p-value<0.05) are plotted.**

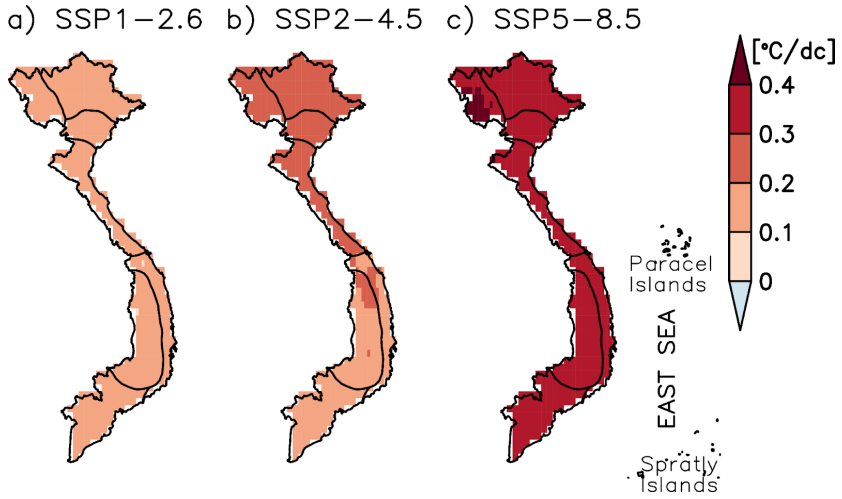

Figure S7. **Trends (day/decade) in the annual number of days (Nm,1) on which daily minimum WBGT (WBGTm) exceeds the Level 1 threshold (>29°C) over Vietnam during the study period (1985–2100) under three Shared Socioeconomic Pathways (a) SSP1-2.6, (b) SSP2-4.5, and (c) SSP5-8.5 (bottom). Only significant trends (p-value<0.05) are plotted.**

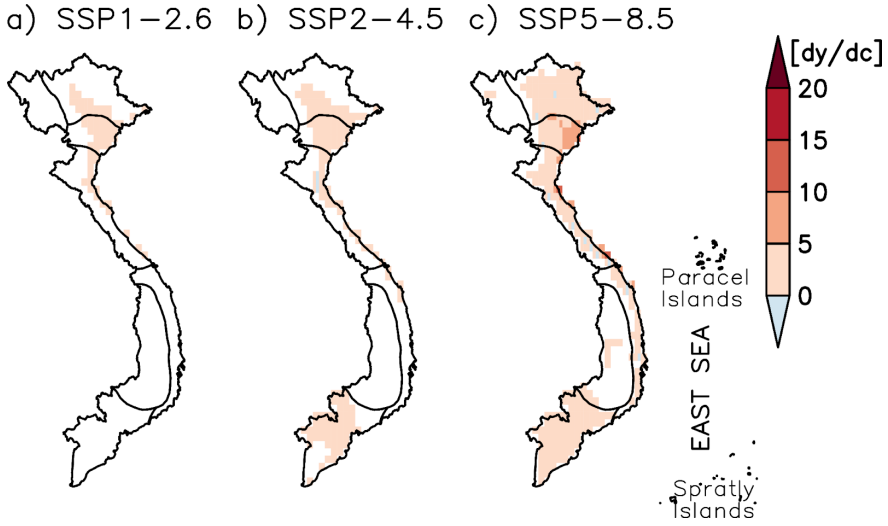

Figure S8. Temporal evolution of annual maximum WBGTm (WBGTm,x), averaged over seven subregions of Vietnam, under three Shared Socioeconomic Pathways: (green) SSP1-2.6, (blue) SSP2-4.5, and (red) SSP5-8.5.

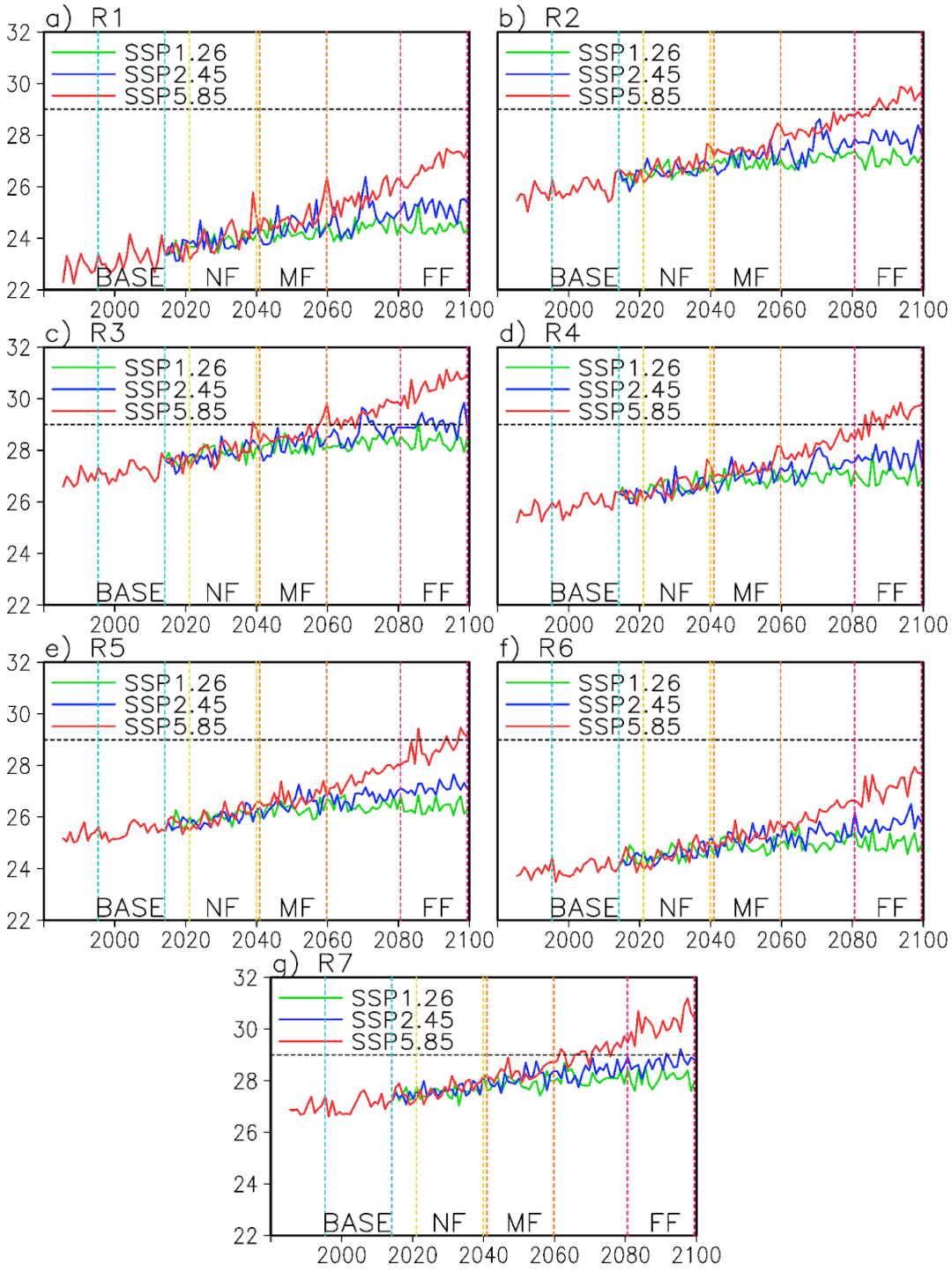

Figure S9. As in Figure S8 but for the number of days per year Nm,1 on which the level 1 threshold of WBGTm is exceeded.

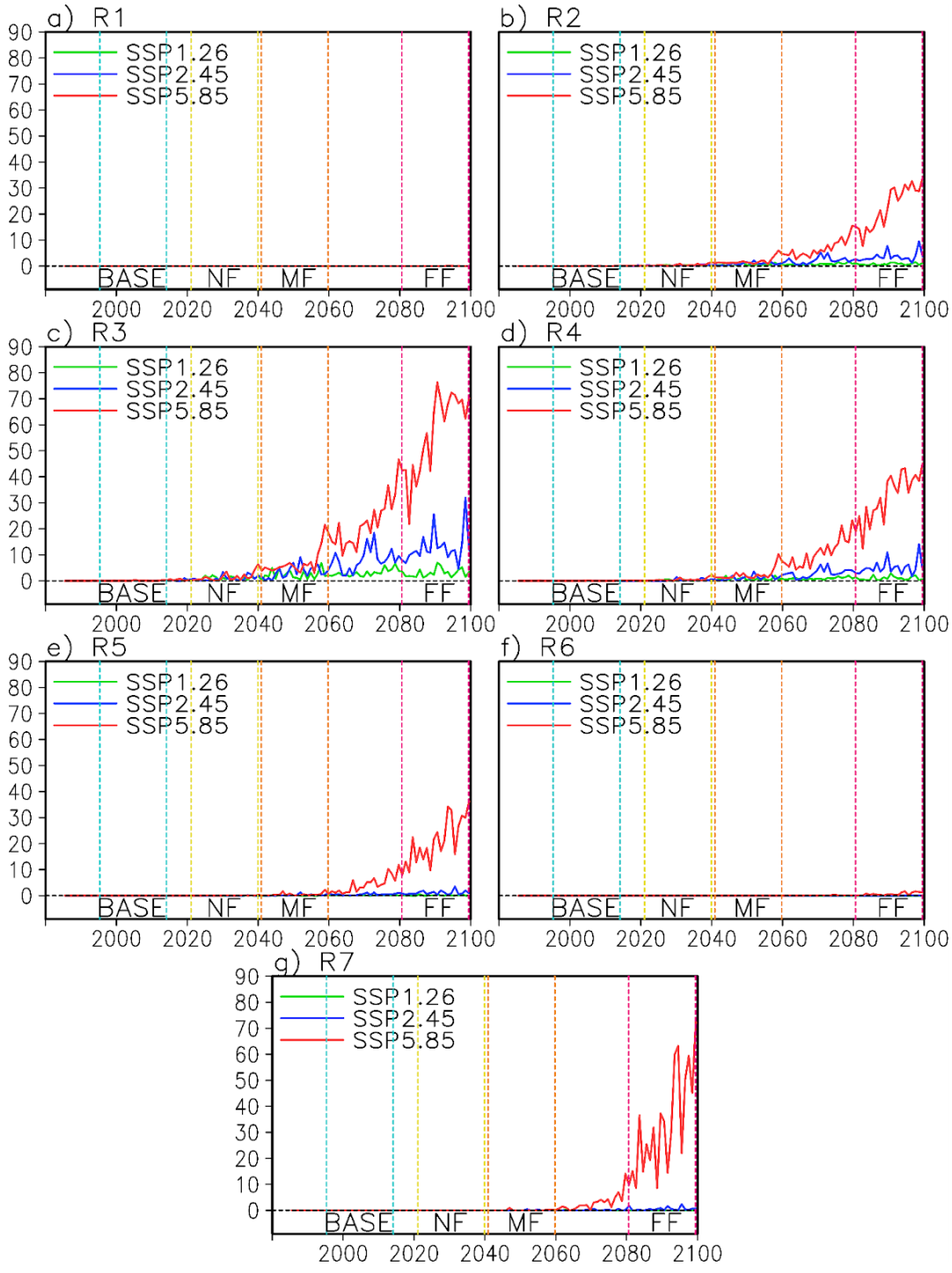

Figure S10. **(a) Differences in annual maximum WBGTm (WBGTm,x) averaged over the seven subregions of Vietnam between GWLs and the baseline period (1995–2014). (b) same as (a), but for the yearly number of days ($N_{m,1}$) when WBGTm exceeds the Level 1 threshold (>29°C).**

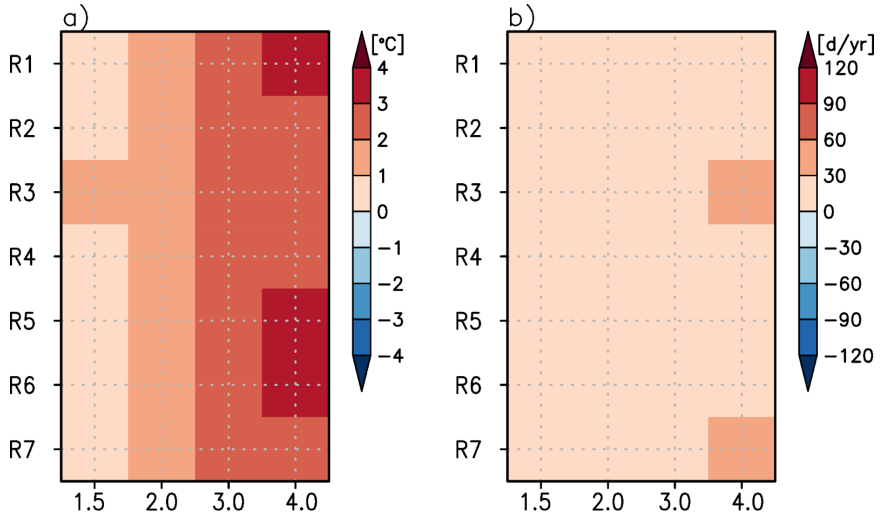

Figure S11. **Biases in annual maximum WBGTm (WBGTm,x) when using simplified WBGT (sWBGT) over Vietnam for (a) the baseline period and the (b), (e), (h) near future (NF; 2021–2040); (c), (f), (i) mid-future (MF; 2041–2060); and (d), (g), (j) far future (FF; 2081–2100) under three Shared Socioeconomic Pathways (top) SSP1-2.6, (middle) SSP2-4.5, and (bottom) SSP5-8.5. Only significant differences (p-value<0.05) are plotted.**

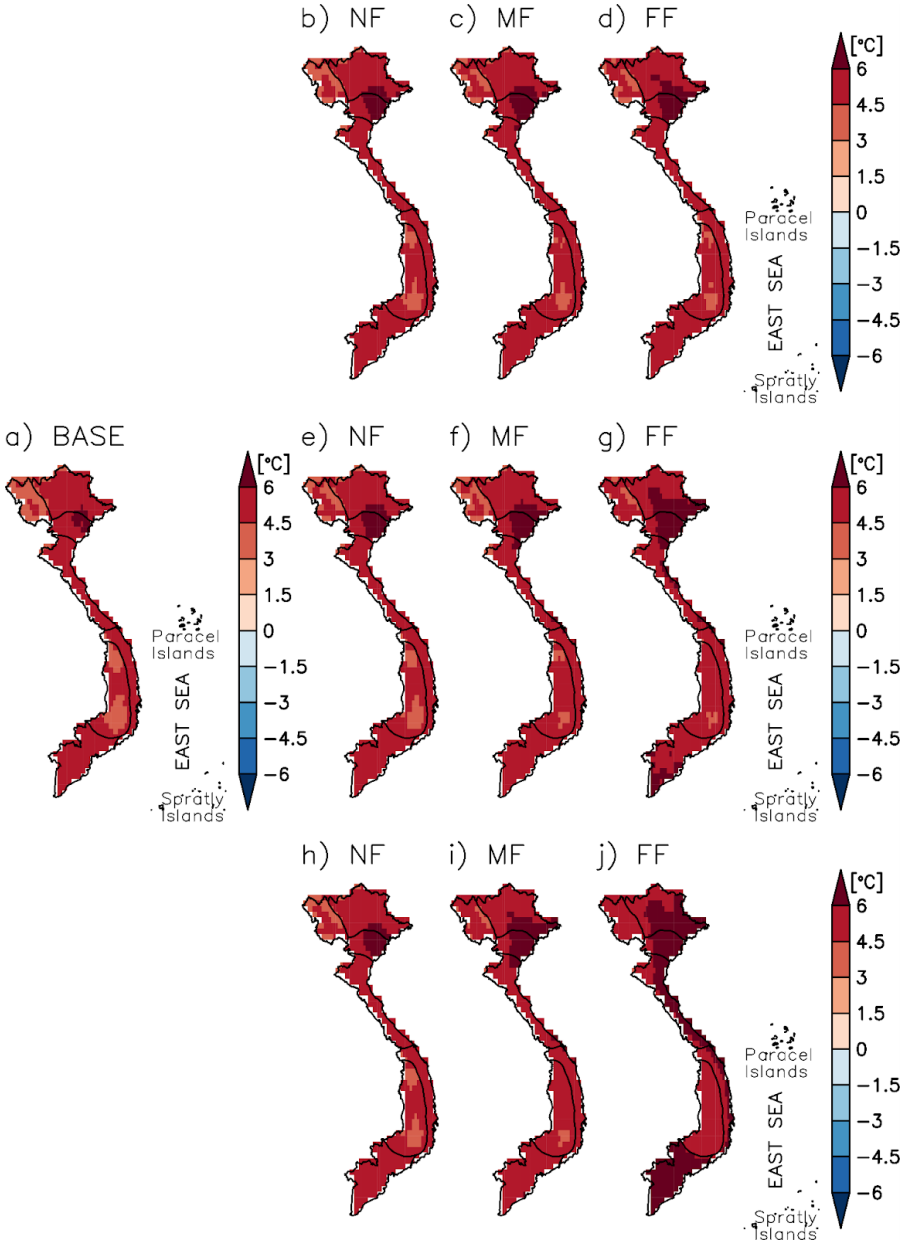

Figure S12. **As in Figure S11 but for the annual number of days (Nm,1) on which daily minimum WBGT (WBGTm) exceeds the Level 1 threshold (>29°C).**

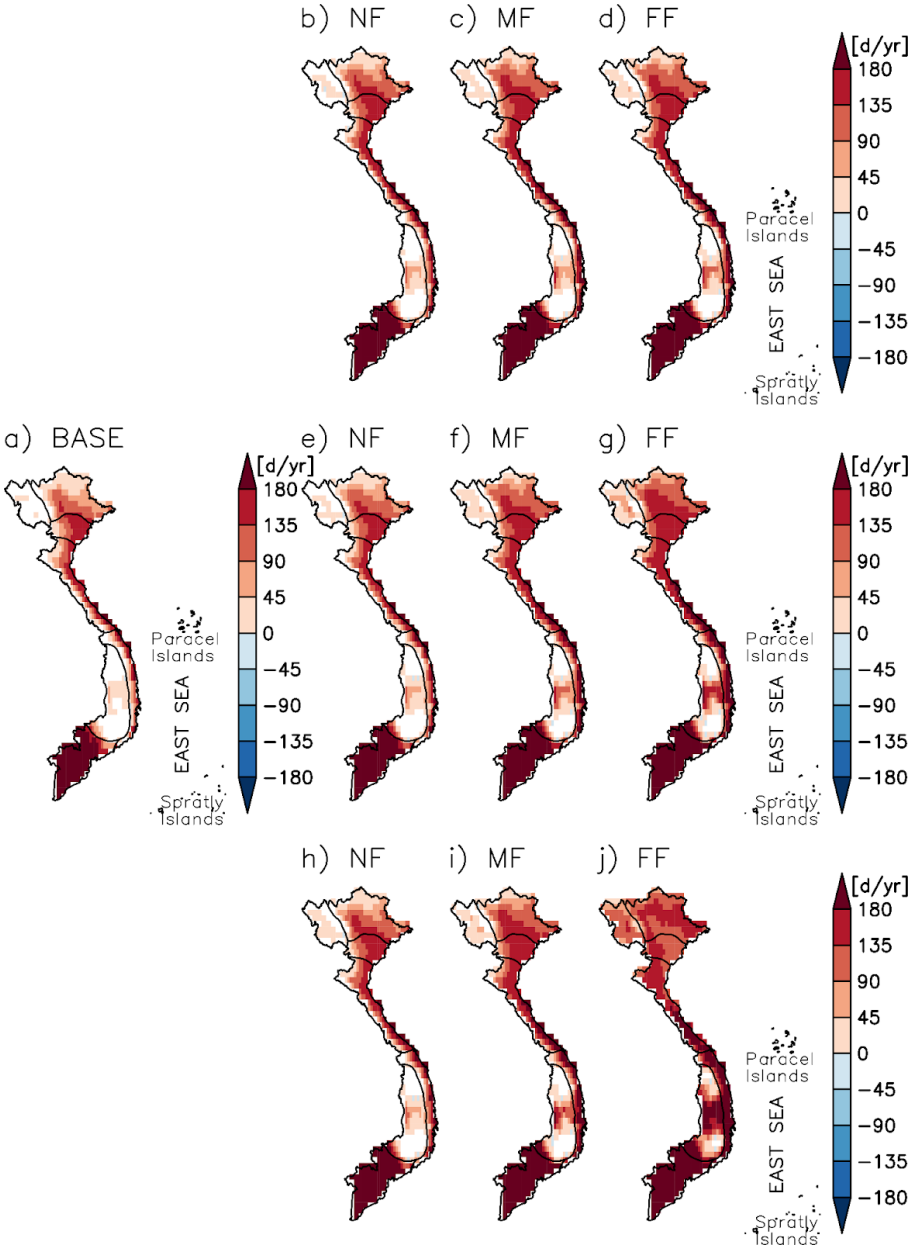

Agence française
de développement
5, rue Roland Barthes
75012 Paris I France
www.afd.fr

What is AFD?
Éditions Agence française de développement publishes analysis and research on sustainable development issues. Conducted with numerous partners in the Global North and South, these publications contribute to a better understanding of the challenges faced by our planet and to the implementation of concerted actions within the framework of the Sustainable Development Goals.
With a catalogue of more than 1,000 titles and an average of 80 new publications published every year, Éditions Agence française de développement promotes the dissemination of knowledge and expertise, both in AFD's own publications and through key partnerships. Discover all our publications in open access at editions.afd.fr.
Towards a world in common.

Publication Director Rémy Rioux
Editor-in-Chief Thomas Melonio

Legal deposit 2nd quarter 2025
ISSN 2492 - 2846

Graphic design MeMo, Juliegilles, D. Cazeils
Layout Denise Perrin, AFD
Printed by the AFD reprography service

To browse our publications:
https://www.afd.fr/en/ressources-accueil